Development of a neural network based model for predicting the occurrence of spread F within the Brazilian sector

A thesis submitted in partial fulfilment of the requirements for the degree of

MASTER OF SCIENCE

of

Rhodes University

by

Masimba Wellington Paradza

June 2008

Abstract

Spread F is a phenomenon of the ionosphere in which the pulses returned from the ionosphere are of a much greater duration than the transmitted ones. The occurrence of spread F can be predicted using the technique of Neural Networks (NNs). This thesis presents the development and evaluation of NN based models (two single station models and a regional model) for predicting the occurrence of spread F over selected stations within the Brazilian sector. The input space for the NNs included the day number (seasonal variation), hour (diurnal variation), sunspot number (measure of the solar activity), magnetic index (measure of the magnetic activity) and magnetic position (latitude, magnetic declination and inclination). Twelve years of spread F data measured during 1978 to 1989 inclusively at the equatorial site Fortaleza and low latitude site Cachoeira Paulista are used in the development of an input space and NN architecture for the NN models. Spread F data that is believed to be related to plasma bubble developments (range spread F) were used in the development of the models while those associated with narrow spectrum irregularities that occur near the F layer (frequency spread F) were excluded. The results of the models show the dependency of the probability of spread F as a function of local time, season and latitude. The models also illustrate some characteristics of spread F such as the onset and peak occurrence of spread F as a function of distance from the equator. Results from these models are presented in this thesis and compared to measured data and to modelled data obtained with an empirical model developed for the same purpose.

Acknowledgements

I wish to extend my sincere gratitude to my supervisors Dr Lee-Anne McKinnell and Dr Pierre Cilliers for their guidance and unwavering support towards the success of this study.

Thanks to the staff of the Hermanus Magnetic Observatory (HMO) for their hospitality, support and encouragement during my stay at HMO. Thanks to Dr Jonas R. de Souza and Dr M.A. Abdu for the provision of spread F data and the spread F model used for a comparative analysis in this study. The assistance of Mr. Patrick Sibanda with Matlab programming is gratefully acknowledged. Special thanks goes to NASSP, the University of Cape Town and Rhodes University.

My sincere thanks to my wife and daughter for their patience, understanding and much more. Thanks to all my coursemates (Fred Joe, Chigo, Stefan and Jean), friends and colleagues who assisted me in many ways.

To God be the glory.

Contents

List of Figures

List of Tables

Chapter 1

Introduction

Spread F is a phenomenon of the ionosphere in which the pulses returned from the ionosphere are of a much greater duration than the transmitted ones. It can be observed by both radio techniques (e.g. ionosonde, radar, scintillation etc.) and optical techniques (e.g. by observing the F region nightglow emissions using either conventional photometers or wide-angle imaging systems) (Fagundes *et al.*, 1999). It is believed to be due to scattering from multiple irregularities at differing ranges and zenith angles. The equatorial and low latitude ionosphere is highly dynamic, which makes it difficult to predict the occurrence of spread F on a night to night basis (Le *et al.*, 2003).

Based on spectral characteristics, ionospheric irregularities of scale sizes ≥ 20 km have been termed as large scale, those between 100 m and 20 km as intermediate scale and those between 10 m and 100 m as transitional scale while those < 10 m are referred to as small scale irregularities. Irregularities of sizes ranging from 100 m to a few kilometres (intermediate) give rise to spread F as seen on ionograms (Subbarao and Murthy, 2006). Thus, an ionosonde provides the minimum detectable threshold for recording occurrences of spread F. It is observed as a stretching in frequency (frequency spread F) or a stretching in time (range spread F) on an ionogram trace. Due to the way in which spread F is detected by an ionosonde, it can be quantified in terms of its appearance on the ionogram trace or its probability

of occurrence. In this study I have focused on the probability of occurrence since it is the parameter of most interest in the prediction of spread F. This work is complimentary to the work of Abdu *et al.* (2003), referred to as the Brazilian group in this thesis.

Spread F affects radio communication and navigation systems utilising the Earth-Space propagation path, and is most often observed at the equatorial latitudes. Spread F is studied because of its strong influence on trans-ionospheric radio-wave communication (Fagundes *et al.*, 1999; Ossakow, 1981; Hysell and Shume, 2002).

A problem which has persisted since equatorial spread F was first detected in ionosonde data is that the onset of the spread phenomenon is difficult to predict from night to night (Huang and Kelley, 1996). Furthermore, the randomness in spread F occurrence prevents the systematic observation of the formation of bubbles necessary for making progress in their prediction. In order to understand this phenomenon, there is a need to develop nowcasting and forecasting techniques (Sultan, 1996).

Spread F also disrupts radio signals from astronomical sources; predictions from a spread F forecasting model may be used to reschedule observing times. A spread F occurrence model will go a long way towards reducing the amount of work required in order to make corrections for radio astronomy data. The model developed in this study will be applicable to all radio communication predictions as well as general radio science where the ionosphere is utilised.

This study aims to develop a neural network (NN) based model for predicting the occurrence of spread F for the Brazilian region. The Brazilian stations are Fortaleza and Cachoeira Paulista, they are within the equatorial anomaly region. The objectives of this research included the study of the spread F phenomenon, specifically the cause and effect relationships and its variability. The intention was to come up with a suitable input space for the NN. The second objective was to study the principle of NN modelling

technique in order to decide on the NN type applicable for this reasearch.

This thesis consists of six chapters. Chapter 1 presents the aim and the relevance of this study. Chapter 2 gives the theoretical background of spread F phenomenon and its variability, and provides some ionogram images showing the presence of different types of spread F. Chapter 3 gives a brief introduction to the basic literature on the NN technique as applied to this study. Chapter 4 provides the source and an interpretation of spread F data. It presents an initial attempt to determine the optimum parameters for the input space for an initial single station NN model. The resulting initial NN model is further developed to give the single station models for Fortaleza and Cachoeira Paulista stations in Brazil. The results from these models are presented and discussed. In Chapter 5, the development of the Brazilian sector NN (BSNN) model is outlined and the results are presented and discussed. An error analysis is performed in order to account for some cases where the BSNN model does not perform very well. A comparative analysis of the BSNN model results and the results of an empirical model (Abdu *et al.*, 2003) is performed for some selected months during 1989 and the results are presented and discussed. The discussions and conclusions for this study are given in Chapter 6.

Chapter 2

Background Theory

2.1 Introduction

This chapter reviews the literature on the spread F phenomenon, the cause and effect relationships of spread F irregularities, the basic plasma processes governing the generation of the plasma bubble and associated plasma irregularities, and the variability of spread F.

2.2 The spread F phenomenon

Spread F (equatorial spread F, ESF) is a generic name given to plasma irregularities with a wide spectrum of scale sizes that occur during the night in the equatorial F region ionosphere. These plasma density fluctuations range from tens of centimetres to hundreds of kilometres. ESF is mainly generated through the gravitational Rayleigh - Taylor (R-T) instability in conjunction with other physical processes.

Plasma density depletions are well known features of ESF, and are believed to emerge after the development of a R-T instability on the bottomside of the F layer; they are identified as the stretching out in frequency (frequency spread F) or in time (range spread F) on an ionogram trace for the echo pulse reflected from the F2 layer (Cecile *et al.*, 1996; Chen *et al.*, 2006; Huba *et al.*,

1996; Le *et al.*, 2003; Lee *et al.*, 2002; Bowman and Mortimer, 2002; Huang *et al.*, 2002; Kelly *et al.*, 2002; Sastri, 1999; Fagundes *et al.*, 1999; Haldoupis *et al.*, 2003).

2.2.1 The equatorial ionosphere

A unique geometry exists at the magnetic equator in which the ambient ionospheric plasma gradient is both antiparallel (parallel but oppositely directed) to gravity and perpendicular to the magnetic field, coupled with the east-west electric field. This physical arrangement is unstable to small bottomside plasma density perturbations. The configuration of the Earth's magnetic field, which is horizontal at the equator, explains the latitudinal distribution of ESF, which is mostly observed at the equatorial regions and low latitudes (Cecile *et al.*, 1996; Jayachandran *et al.*, 1997; Sultan, 1996).

2.2.2 The Rayleigh - Taylor instability

Consider a finite plasma in a magnetic field under gravity as shown on the right in Figure 2.1 below. The action of the force of gravity on the electrons and ions causes them to drift parallel to the boundary (Das, 2004). A per-

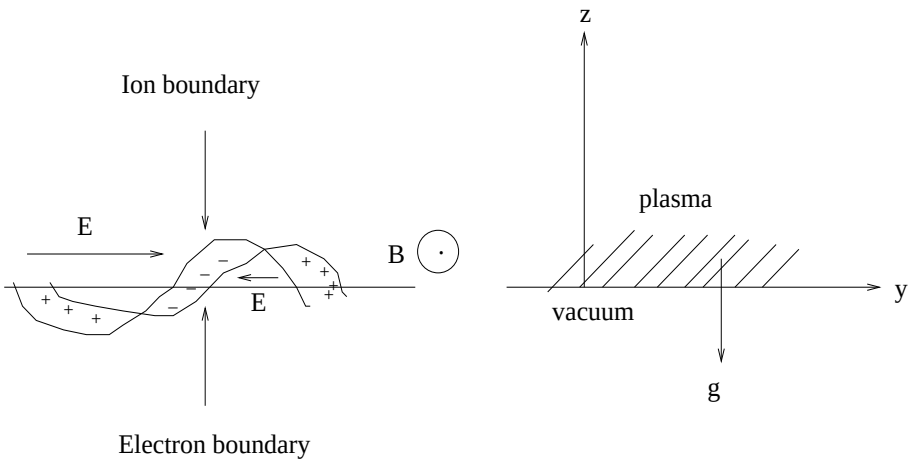

Figure 2.1: Rayleigh-Taylor instability schematic diagram (Das, 2004, page 107).

turbation of the interface between the fluids causes the plasma density to make sinusoidal variations in the z direction. The direction of the magnetic field is out of the paper as indicated in Figure 2.1. Because of drifting, the ion and electron boundaries are separated out, and this gives rise to electric fields as indicated on the left in Figure 2.1. Thus, an ExB drift is produced in the opposite direction amplifying the initial perturbation (Cecile *et al.*, 1996).

When such a disturbance moves on the surface of the interface in the form of a wave, they generate so-called gravity waves and these provide a seed mechanism for the R-T instability. When gravity waves propagate perpendicular to the magnetic field, they generate a polarisation electric field, and these are amplified nonlinearly by the R-T instability (Huang *et al.*, 2002).

The basic plasma fluid equations of continuity, motion, and current continuity can be combined to give the local linear growth rate for such instabilities. The linear growth rate for the collisional R-T instability is given by Kelley (1989):

$$\gamma = \frac{g}{\nu_{in}} \frac{1}{n_0} \frac{\partial n_0}{\partial h}. \tag{2.1}$$

In equation 2.1 n_0 is the background electron density, h is the height above the earth, ν_{in} is the ion-neutral collision frequency, and g is the gravitational acceleration (positive downwards). This expression gives the basic ionospheric conditions necessary for the ESF occurrence. The growth rate γ is greatest when the peak height (h_{max}) of the ionosphere is high, which maximises the g/ν_{in} term when the bottomside density gradient is sharp. This usually takes place after local sunset. The day-to-day variability of ESF is probably related to atmospheric effects like gravity waves which are capable of triggering an R-T instability, while transequatorial thermospheric winds tend to impede the development of the instability (Cecile *et al.*, 1996; Huang and Kelley, 1996; Kelley, 1989; Sultan, 1996).

2.2.3 The generation of plasma bubbles

After sunset at the equatorial regions, the F layer rises under the effect of an enhanced eastward electric field resulting from the recombination processes. Ions and electrons undergo gravitational drift leading to charge separation. The collisions between the plasma constituents and neutrals tend to impede the separation, and hence the F Layer has to reach altitudes for which the ion-neutral collision frequency is sufficiently small to allow the development of the instability. In the presence of an initial perturbation the instability develops leading to large scale troughs and enhancements associated with plasma bubbles (Cecile *et al.*, 1996; Sultan, 1996; Huba *et al.*, 1996; Jayachandran *et al.*, 1997).

During an ESF event, it is believed that high plasma density magnetic flux tubes at the bottomside of the ionospheric F region change places with lower density flux tubes from below in a way that is analogous to the hydrodynamic R-T instability. The height and vertical drift velocity of the bottomside of the F region are the deciding factors for the onset of ESF, with maximum growth rate occurring at the moment of peak height (Sultan, 1996). ESF onset conditions fall into two categories:

(a) dynamic parameters:

These include magnitudes of electric fields (plasma drifts) and neutral wind velocities.

(b) factors describing the distribution of plasma:

These factors include the distribution of plasma and neutrals locally and along magnetic flux tubes. In addition to the presence of the "seed" mechanism, magnetic activity, solar cycle, neutral winds, vertical plasma drift, F region peak height, local time and time of year are important parameters in predicting ESF. The vertical plasma drift is the initial source of free energy that allows the R-T instability process to occur. According to Huang and Kelley (1996) gravity waves are a very effective seed mechanism for the production of ESF bubbles, and the height of the F layer is an important factor for the onset of ESF.

The prereversal enhancement of eastward electric fields moves the F layer to a higher and more unstable altitude. Variations in the electric field strength, and the parameters of gravity waves, such as amplitude, frequency and wavelength, change from time to time resulting in a variability in ESF. Gravity waves propagating with an azimuthal angle range of about 10° relative to the zonal direction are expected to be capable of initiating R-T instability resulting in plasma bubbles (Huang and Kelley, 1996).

2.2.4 Range and frequency spread F

As mentioned in the preceding section, range type spread F (RSF) is associated with developing, or developed, plasma bubble events. Frequency type spread F (FSF) is associated with narrow spectrum irregularities that occur near the peak of the F layer, and are not due to unstable, or potentially unstable, flux tubes (Abdu *et al.*, 2003).

An ionosonde radiates short pulses of high frequency radio waves upward, these waves are reflected from the ionosphere and are recorded as traces on ionograms. As presented in figures 2.2 to 2.5, spread F can be best quantified by its appearance on an ionogram or by a measure indicating the presence or absence of spread F. For the purposes of this study, a measure equal to one was assigned to spread F presence and a measure equal to zero for spread F absence.

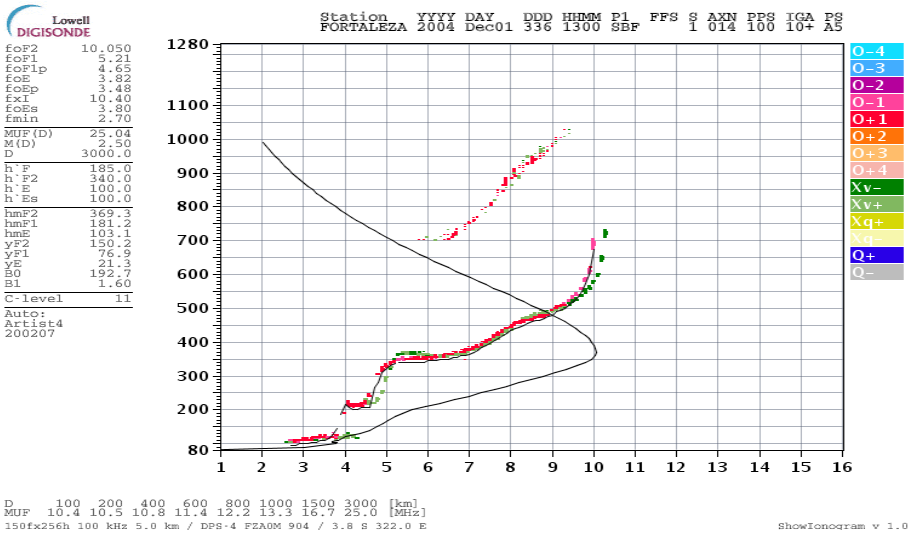

Figure 2.2: An ionogram image showing the appearance of the ordinary (in red) and extrordinary (in green) traces when there is an absence of spread F. Source (http:/ /car.uml.edu:8080/common/DIDBFastStationList).

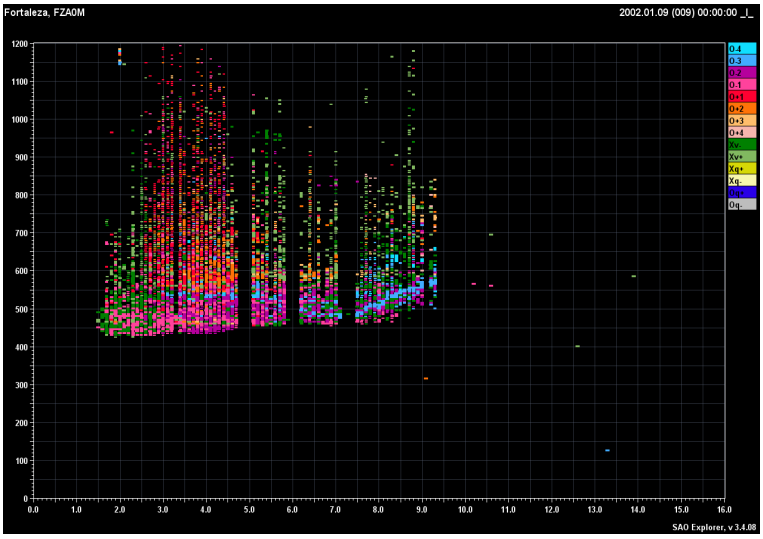

Figure 2.3: An ionogram image showing the appearance of the ordinary and extrordinary traces due to the presence of range spread F. Ionogram image provided by the Brazilian group.

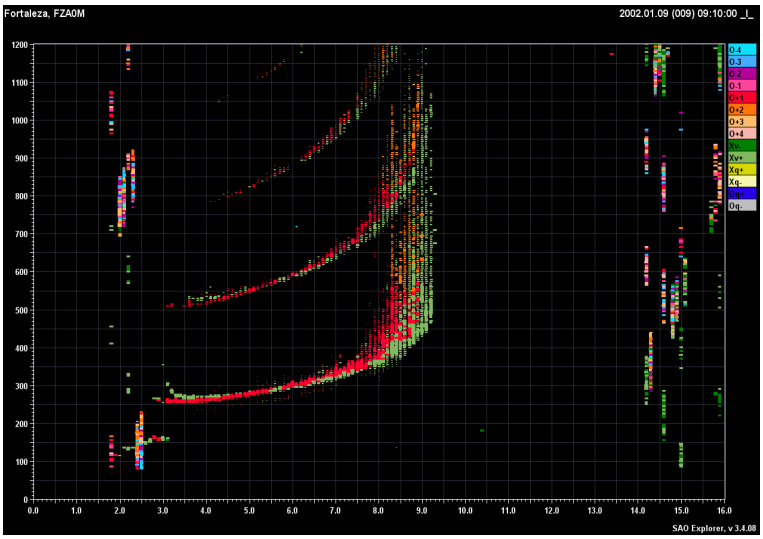

Figure 2.4: An ionogram image showing the appearance of the ordinary and extrordinary traces due to the presence of frequency spread F. Ionogram image provided by the Brazilian group.

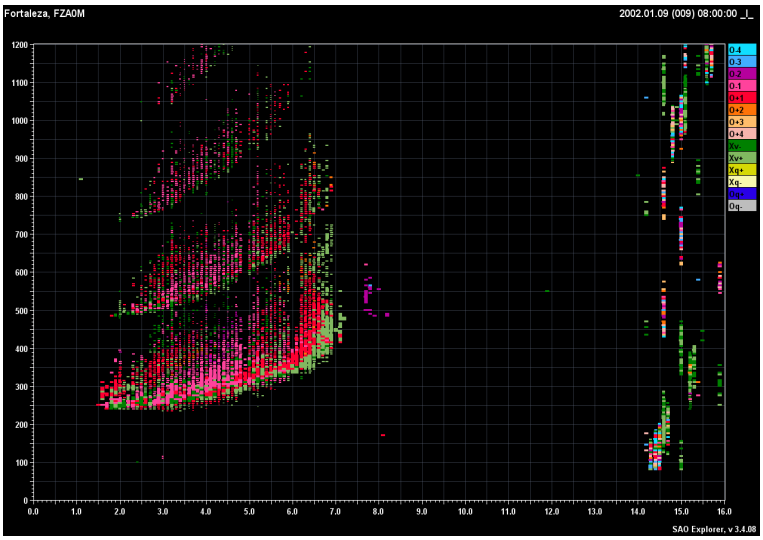

Figure 2.5: An ionogram image showing the appearance of the ordinary and extrordinary traces when there is a mixture of both range and frequency spread F. Ionogram image provided by the Brazilian group.

2.3 Variability of spread F

The occurrence of ESF is linked to magnetic declination, geomagnetic activity, time of day, time of the year, sunspot number and latitude, among other factors. The variability in spread F is explained in brief detail in the following subsections. An understanding of variability in spread F gives a lead into the parameters that have to be considered in coming up with the NN input space.

2.3.1 Geomagnetic activity

At equatorial regions spread F occurs on magnetically quiet days and disappears with the onset of a magnetic storm, whereas at middle latitudes spread F is essentially a storm phenomenon (positively correlated with magnetic storm activity). However, spread F can be generated when the magnetic storm is onset near evening hours. Near the magnetic equator the occurrence of spread F is negatively correlated with magnetic activity. Near solar maximum, geomagnetic activity strongly disrupts spread F activity before local midnight. The post-midnight onset of spread F is not entirely due to the destabilisation of local plasma but may result from plasma irregularities that were generated earlier to the west of the observation region and drifted onto the signal path (i.e. an overhead passage of irregularity patches that formed from elsewhere) (Sastri, 1999; Davis, 1990; Hysell and Shume, 2002).

2.3.2 Diurnal variations

The magnetic field lines at equatorial F region heights are mapped to the lower and higher latitudes; and, during the daytime, the high plasma conductivity of the E region will suppress any electric field inhibiting the development of the plasma instability. However, after sunset, the E region conductivity drops considerably and the electric fields generated at the bottomside of the F region can develop plasma instabilities. The rapid uplifting of the F region just after sunset is one of the important conditions for the onset of ionospheric plasma irregularities. Fluctuations in the ion drift velocity

or plasma density, caused by gravity waves or other large scale structures, can act as the seed for the generation of the initial perturbation (Fagundes *et al.*, 1999). It therefore follows that spread F is predominantly a night-time phenomenon.

2.3.3 Seasonal variations

Near the magnetic dip pole there is a region of permanent spread F where during the summer, spread F occurs 90-100% of the time at night and 50-60% around noon. During winter in this region, no diurnal variation is observed, and spread F occurs almost 100% of the time both day and night (Davis, 1990). ESF is seasonally controlled and irregularity events occur preferentially during times of the year when the local magnetic meridian and the sunset terminator are aligned, a situation which maximises the prereversal enhancement of vertical plasma drift near the magnetic equator (Jayachandran *et al.*, 1997). At equatorial latitudes spread F occurs mostly near the equinoxes, or during local summer, at longitudes where the geographic and magnetic dip equators are far apart (e.g. in South America).

2.3.4 Geographical variations

At the equatorial regions, spread F occurs invariably during the night while at high latitude regions it occurs mainly during the night but occasionally during the day. Equatorial spread F occurs at latitudes bounded by $\pm 20°$, and high latitude spread F begins at about 40° geomagnetic latitude; its probability of occurrence increases with latitude. There is little spread F occurrence at geomagnetic latitudes between 20° and 40° (Davis, 1990).

2.3.5 Sunspot dependence

Subbarao and Murthy (2006) established that ESF, as observed on an ionogram, shows a positive correlation with solar activity in the Indian zones. Near the magnetic equator the sunspot influence appears through the effect of magnetic disturbance on spread F and there is a strong negative correlation

at sunspot maximum between the appearance of spread F, and the magnetic disturbance disappears in years of low solar activity. Near the geomagnetic equator, spread F is an evening and night-time phenomenon beginning near sunset and having a most likely occurrence between 21:00 LT and 01:00 LT, being earlier at sunspot maximum (Davis, 1990).

2.3.6 Summary

The background theory on spread F phenomenon and variability in spread F has been presented. Additional detail on the spread F phenomenon can be obtained in the references provided in this chapter.

Chapter 3

Neural Networks

3.1 Introduction

This chapter presents the basic literature on neural networks (NNs) and the way in which one can determine the NN architecture and the optimum parameters for the NN input space.

Artifical Neural Networks, referred to in this thesis as neural networks (NNs), are information processing systems that have performance characteristics which are analogous to biological neural networks and they are modelled after the human brain. They compute relationships between a given set of input(s) and known output(s) as described in Haykin (1994).

NNs can be used to develop empirical models since they extract patterns and detect trends that are too complex to be detected by classical methods (Williscroft and Poole, 1996). NNs have been successfully applied to medicine, speech production, pattern recognition, control systems and business (Fausett, 1994); and ionospheric prediction e.g McKinnell and Poole (2003).

3.2 Basic elements of a neural network

A neuron is an information processing unit with three basic elements; namely, a set of synapses, an adder and an activation function, and it is fundamental to the operation of a NN.

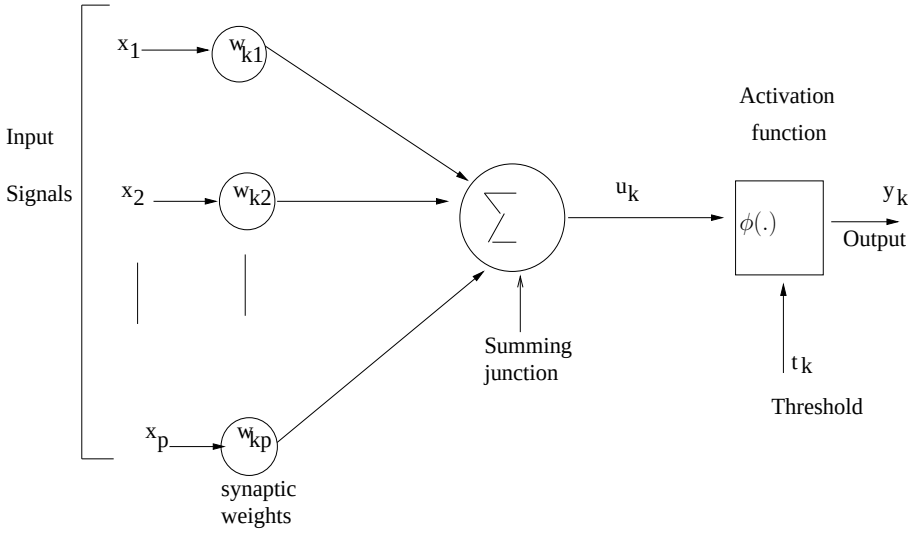

Figure 3.1: Nonlinear model of a neuron (Haykin, 1994, page 8).

Figure 3.1 shows a basic model of a neuron, where an input signal x_j at the input of synapse j ($j = 1, 2...., p$) connected to a neuron k is multiplied by the synoptic weight w_{kj}. The weights are positive when the synapse is excitatory and negative when it is inhibitory (Haykin, 1994). All the weighted signals are summed up by the adder (summing junction). The activation function $\phi(.)$ is responsible for limiting the amplitude of the output of the neuron and a threshold or bias (applied externally) is included to increase or decrease the net input of the activation function.

Typically, an activation function is a non-linear function; examples include the binary threshold function, bipolar threshold function and a sigmoid function. For the purpose of this work, a neuron activation function with a slope

parameter of unity

$$f(x) = \frac{1}{1 + e^{-x}} \tag{3.1}$$

where f(x) is the binary sigmoid function was used. The above function is both differentiable and continuous which is a key consideration in choosing activation functions for a backpropagation algorithm.

3.3 Network layers

There are three types of neuron layers: input, hidden and output layer.

- The **input** unit presents the raw information that is fed into the network.
- The **hidden** unit's activity is determined by the activities of the input units and weights on connections linking them.
- The **output** unit's activity depends on the activities of hidden units and the weights linking them.

The weighted connections linking the layers can be classified as feedforward, feedback, lateral and time delay depending on the way in which data propagates from lower neuron layers upward. For feedforward connections, data from neurons of a lower layer are propagated in the forward direction to neurons of an upper layer.

3.4 Training, validating and testing

A NN is trained using data which contains known input and output parameters. The purpose of training is to allow the NN to learn the relationship between a given set of inputs and the known output.

The data is arranged into the training, validating and testing sets. The training set is used for training the NN, the validating set, is used to ascertain the performance of the NN on patterns that are not part of the training

dataset and the testing set is used to assess the final overall performance of the NN. The weights are selected at random and training is then performed by adjusting these weights in the dataset iteratively using a training algorithm. The error development graph is monitored to avoid over-training of the NN which may lead to memorisation instead of generalisation of the patterns learnt (Fausett, 1994).

3.5 Single and multilayered networks

A single layered network has one layer of connection weights or nodes (hidden layers) while a multilayered network has more layers of nodes between the input and output units. A multilayered network has an advantage over a single layered network in that it can solve more complicated problems than single-layer nets. Multilayered networks can perform a non linear mapping from an n dimensional input space to an m dimensional output space (Fausett, 1994).

3.6 Supervised versus unsupervised learning

Adaptive networks are those which are able to change their weights during training. The learning methods in adaptive networks can be classified into two categories, namely supervised and unsupervised learning.

Supervised learning is achieved by presenting a sequence of training vectors, each with an associated output target vector. The weights are then adjusted according to a learning algorithm. For **unsupervised** training, self organising networks group similar input vectors together without the use of training data to specify what a typical member of each group looks like. They modify the weights in such a manner that the most similar input vectors are assigned to the same output unit (Fausett, 1994).

3.7 Backpropagation neural network

The training method called backpropagation of errors is a gradient descent method which works on the principle of minimising the total squared error of the output from the NN. A backpropagation network is a multilayered, feedforward network trained by backpropagation. The backpropagation algorithm can be summarised as follows:

The input unit receives an input signal in a forward pass and sends it to each of the hidden units. Each hidden unit then computes an activation function and sends its signal to each of the output units. Each output unit computes its activation function which then forms the response of the network. At this stage, each output unit compares its computed activation with its target so as to determine the error for that unit. A factor comprising all the errors for each output unit is computed and distributed back to the previous units. In the same fashion, another factor is computed for the hidden units. These factors are then used to adjust the weights for all units until a minimum set error is achieved (Fausett, 1994).

It follows that the backpropagation algorithm involves three stages, which are the feedforward of the input training pattern, the calculation and backpropagation of errors, followed by the adjustment of weights. For the purpose of this work, a standard backpropagation NN was used. The main reason for this is its ability to give good responses to input that is similar but not identical to that used in training (generalisation) (Fausett, 1994).

3.8 Root Mean Square Errors (RMSE)

The method for determining the optimum NN architecture and input space is the RMSE defined by:

$$RMSE = \sqrt{\frac{1}{N}\sum_{i=1}^{N}(X_{pred} - X_{meas})^2}. \tag{3.2}$$

where N is the number of data points, X_{pred} represents the data predicted by the model while X_{meas} represents the measured data. A combination of parameters that provided the least RMSE is considered to be the optimum network for perfoming the required predictions. This method has been successfuly used in ionospheric studies, e.g. Habarulema *et al.* (2007).

3.9 NN software

The Stuttgart Neural Network Simulator (SNNS) developed by the Institute for Parallel and Distributed High Performance Systems, University of Tübingen, and the Wilhelm-Schickard-Institute for Computer Science in Germany was used in the development of this model. The software is distributed by the University of Tübingen at (http://www.ra.cs.uni-tuebingen.de/SNNS/).

3.10 Summary

An introduction to the basic literature on NN has been presented. This chapter should, however, not be regarded as a complete review of the literature on NNs, but as an introduction to NN only sufficient to give the reader of this thesis an idea on NN as applied to this research. More information on NNs can be obtained in the references provided in this chapter.

For the purpose of this research, an adaptive, multilayered, standard feed forward NN with backpropagation learning algorithm was used.

Chapter 4

Single station models

This chapter outlines the development of single station models. An initial attempt at predicting spread F using NNs is presented first, followed by the Fortaleza and Cachoeira Paulista single station models. The source and interpretation of spread F data is provided together with details of the development of the optimum network. The results from the initial, Fortaleza and Cachoeira Paulista single station models are presented and discussed.

4.1 Development of the initial single station model

Brazilian spread F data (Abdu *et al.*, 2003) was used to develop the models presented in this thesis. Initially a single station model based on data from the Brazilian station Fortaleza (3.9°S, 38.45°W, dip angle: -9°) was developed. Twelve (12) years worth of data from 1978 to 1989 inclusively were used in the study. An example of a monthly data file is shown in Table 4.1.

Table 4.1: Spread F data format

01-02 RRRRRRRRRRRRRRRRRMMMMMMMMMMMM
02-03 RRRRRR RRRRRRRRRRRRMMMMMMMMMMM
05-06 FFMRRRRRRRRRRRRRRRRRRRRCCCCC
08-09 RRRRRRRRRRRRRRRRRMMMMMMMMMMM
21-22 RRRRRR RRRRRRRRRRRMMMMMMMMMMM
25-26 FFMRRRRRRRRRRRRRRRRRRRCCCCC
30-31 CCCCCCCCCCCCCCCCCCCCCCCCCCCCCC
31-01 CCCCCCCCCCCCCCCCCCCCCCCCCCCCCC

Table 4.1 shows the format of the spread F data files where the letters denote range spread F (R), frequency spread F (F) and mixture of the two (M). The letter C indicates that there was an absence of data (due to equipment failure or other causes). The blank spaces indicates that neither a mixture, range or frequency spread F occurred. The data was sampled at fifteen minute intervals from 18:00 LT to 08:00 LT the following day. Due to the way in which spread F is detected by an ionosonde, it can be quantified in terms of its appearance on the ionogram trace (as denoted by the letters) or its measure of occurrence. When spread F is present, the measure of spread F occurrence is denoted by a 1 and an absence of spread F is denoted by a 0. Computer programs were designed in MATLAB to read the monthly data files and arrange the data into the corresponding year, day number, time and a measure of spread F (mixture, range, frequency spread F) for both stations (Cachoeira Paulista and Fortaleza).

4.1.1 NN parameters and NN input space

As discussed in chapter 2, local time, season, foF2, magnetic declination and inclination, latitude, F2 layer height (hmF2), solar and magnetic activity are possible factors affecting the occurrence of spread F. Other factors include thermospheric winds, the equatorial ionisation anomaly, the vertical plasma drift and the ExB drift velocity. In ionospheric studies the solar and mag-

netic activity are usually represented by the sunspot number and Ap index respectively.

The input space was developed from a selection of the parameters mentioned above that are known to affect the occurrence of spread F. The consideration of a single station (Fortaleza station for the initial model) implies that only the local time (Hr), season (DN), solar and magnetic activity parameters can be included in the input space. The geographic coordinates are superfluous for single station models and the peak parameters (foF2, hmF2) were left for future investigation. The seasonal and diurnal variations are represented by the day number (DN) and hour (Hr), and were each split into two components to allow data continuity (Williscroft and Poole, 1996) as follows:

$$DNS = sin\left(\frac{2\pi \times DN}{365.25}\right) \qquad DNC = cos\left(\frac{2\pi \times DN}{365.25}\right) \tag{4.1}$$

$$HrS = sin\left(\frac{2\pi \times Hr}{24}\right) \qquad HrC = cos\left(\frac{2\pi \times Hr}{24}\right) \tag{4.2}$$

where DNS, DNC, HrS and HrC are the sine and cosine components of DN and Hr respectively. In the above equations, the normalisation of DNS and DNC to 365.25 takes into consideration the fact that some of the data used was for leap years (Williscroft and Poole, 1996). This helps the NN to view adjacent years as different cycles as well as avoiding a step jump from day 365 (i.e 31^{st} December) to day 1 (i.e 1^{st} January of the following year). The same applies to HrS and HrC for adjacent days. The solar activity is represented by sunspot number (daily sunspot number) and magnetic activity is represented by the Ap index (a three hourly index) for which the historic and present data is readily available. The output parameters were the measure of spread F occurrence (absence and presence), discrete values of ones and zeros representing a measure of presence and absence of spread F respectively. The presence of range spread F, frequency spread F and a mixture of the two as observed on ionograms was treated as ones while the absence of either one of them was treated as zeros, the idea being that the NN will provide a measure of spread F presence and a measure of spread F

absence as outputs.

4.1.2 Root Mean Square Errors (RMSE)

The method for determining the optimum NN architecture and input space is the RMSE defined for the purpose of this work as:

$$RMSE = \sqrt{\frac{1}{N}\sum_{i=1}^{N}\left(SF_{pred} - SF_{obs}\right)^2} \tag{4.3}$$

where N is the number of data points, SF_{pred} is the measure of spread F occurrence predicted by the NN model while SF_{obs} is the measure of spread F occurrence observed on ionograms (observed data). The measure of spread F can be determined as either a measure of spread F presence or spread F absence. A combination of input parameters with the least RMSE is considered the optimum for the measure of spread F predictions.

4.1.3 Determination of an optimum NN architecture

The data used in training the neural networks (NNs) covers the period from 1978 to 1988 inclusively, corresponding to a full sunspot cycle. Initial attempts were made to get the best combination of hidden nodes and hidden layers using data from the two extreme ends of the solar cycle (1979 and 1986 i.e. near solar maximum and near solar minimum respectively). However, the results were inconclusive since the RMSE values differed from one network to the other depending on the years considered. The entire data set was then used for training in an attempt to find an optimum performing NN, i.e. one that will give the least RMSE value. This method has been successfully used in ionospheric studies by Williscroft and Poole (1996).

Table 4.2: Determination of the number of hidden nodes and hidden layers

Nodes in each hidden layer	hidden layers	RMSE value spread F presence	RMSE value spread F absence
10	1	0.376	0.376
15	1	0.374	0.375
20	1	0.373	0.373
30	1	0.371	0.371
30	2	0.370	0.370
30	3	0.370	0.370

Table 4.2 shows the RMSE values obtained in an attempt to determine the optimum NN. In training the NN, the following functions were not changed and they remained the same for all the networks:

- learning function - Standard backpropagation
- Update function - Topological order
- Init function - Randomised weights
- Remap function - none
- The learning parameter was set at 0.001.

The criterion used in determining the optimum combination of hidden layers and nodes for the NN was simply to fix the number of hidden layers and vary the number of hidden nodes. The number of hidden nodes was then fixed at 30, (refer to the above table); and the number of hidden layers varied. From table 4.2, it can be seen that a NN with two hidden layers and thirty hidden nodes in each hidden layer provided the lowest RMSE value and hence an optimum network. Values for 2 and 3 hidden layers are the same, thus, it is

not necessary to have more than two hidden layers.

From Table 4.2, an RMSE of 0.37 can be further reduced by looking for the appropriate representation of parameters for the sunspot number and the Ap index. The procedure for doing so is outlined in the next section. Also from Table 4.2, the RMSE values for a measure of spread F presence and a measure of spread F absence are almost the same, so I then decided to use the measure of spread F presence for the rest of the work that follows from this point onwards. The measure of spread F absence can be used to check for conformity and to verify that the NN performs accordingly. In this

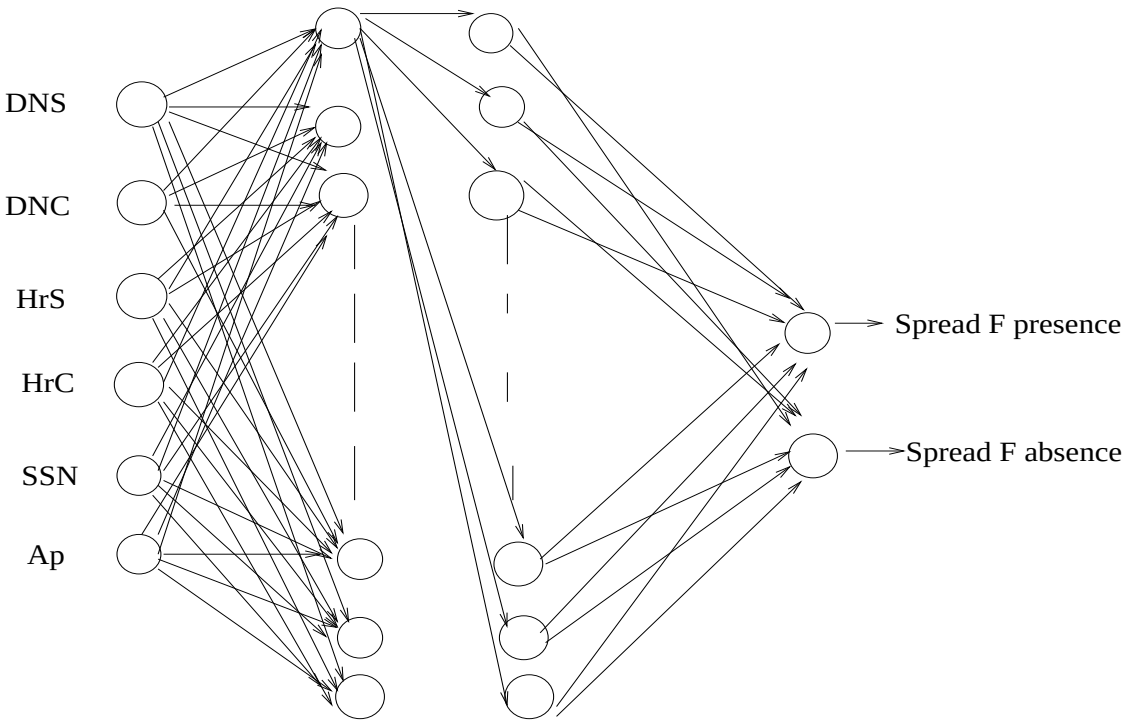

Figure 4.1: The NN architecture for the initial NN model for Fortaleza station.

figure SSN refers to sunspot number (daily values) and Ap is the Ap index (3 hourly values). All connections are not indicated and this figure only serves as an illustration.

4.1.4 Determination of optimum parameters for the NN input space

Previously, during the determination of the NN architecture, I used the daily values for the sunspot number (SSN) and the three hourly values for the magnetic index (Ap). SSN and Ap should be used by the NN, as they are known to affect spread F, but what is not known is the delay that this effect has on the occurrence of spread F. I then used only the seasonal and diurnal parameters as inputs (i.e. DNS, DNC, HrS and HrC respectively) to train a network using data for 11 years, and the resulting RMSE was 0.387 for a measure of spread F presence. This value was larger than the ones obtained when the sunspot and magnetic activity parameters were included as inputs. This confirms statistically that these two (SNN and Ap) can be used as inputs to the NN. This part was done for completeness, since the basic theory on spread F suggests a dependence on magnetic and solar activity.

4.1.5 Sunspot number

A total of eight NNs were trained with five inputs, namely DNS, DNC, HrS, HrC and R_x. The values chosen for x were $0, 0.5, 1, 2, 3, 4, 8$, and 12. R_x is the running mean of the daily SSN calculated over the previous x months. Each network has the same first four inputs (DNS, DNC, HrS and HrC), but differed in the R_x values. The magnetic activity input was excluded at this time.

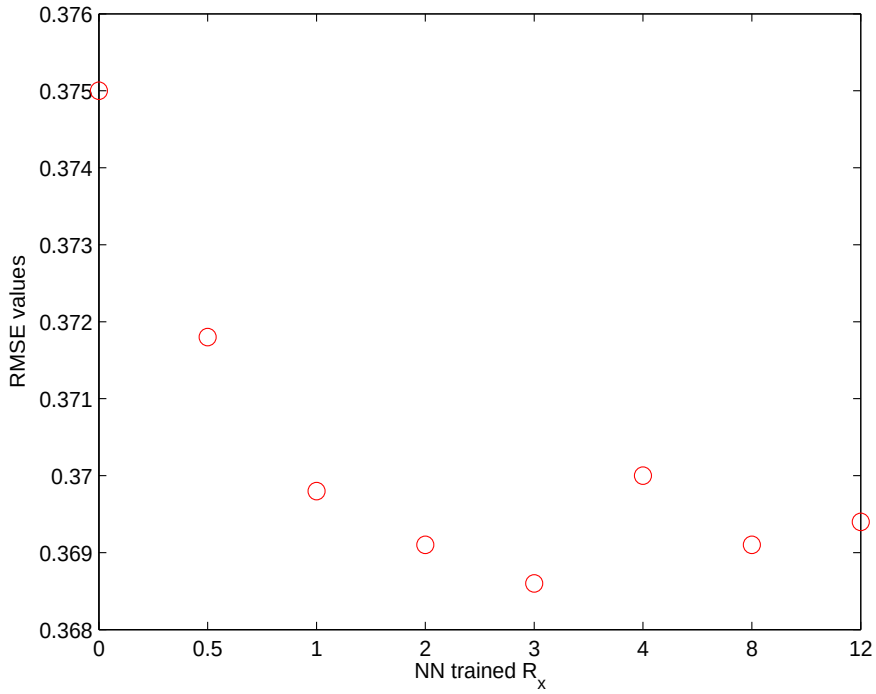

Figure 4.2: A graph showing the RMSE values for each NN trained while attempting to determine the appropriate representation of the solar activity input parameter. In this figure, R_x represents a NN with R_x as one of the inputs.

Figure 4.2 shows the RMSE values between the NN predicted measure of spread F presence and the observed measure of spread F presence during the determination of the appropriate representation for the sunspot number. Each R_x value represent a different NN plotted with the associated RMSE value. The figure illustrates that a NN with R_3 as one of its inputs provided a minimum RMSE value, and is therefore considered optimum for predicting the measure of spread F.

4.1.6 Magnetic activity

A total of six NNs were trained with six inputs, namely DNS, DNC, HrS, HrC and R_3 and A_x. The values of x chosen were $0, 4, 8, 10$ and 32, and A_x represents a running mean of the previous x 3-hourly Ap index values. Each network has the same first five inputs $(DNS, DNC, HrS, HrC, R_3)$, but differed in the A_x values. Figure 4.3 shows the RMSE values between the predicted

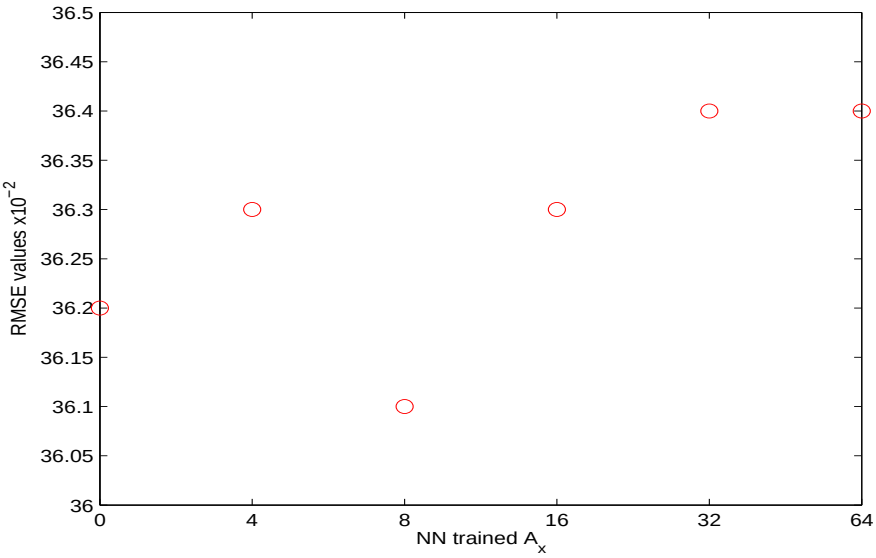

Figure 4.3: A graph showing the RMSE values for each NN trained while attempting to determine the appropriate representation of the magnetic activity input parameter. In this figure A_x represents a NN with A_x as one of the inputs.

measure of spread F presence and the observed measure of spread F presence during the determination of the appropriate representation for the Ap index. Each A_x value represent a different NN plotted with the associated RMSE value. Figure 4.3 illustrates that a NN with A_8 (a running mean over one day of Ap index values) as one of its inputs gives the minimum RMSE value and therefore is the optimum magnetic activity index for predicting the measure of spread F.

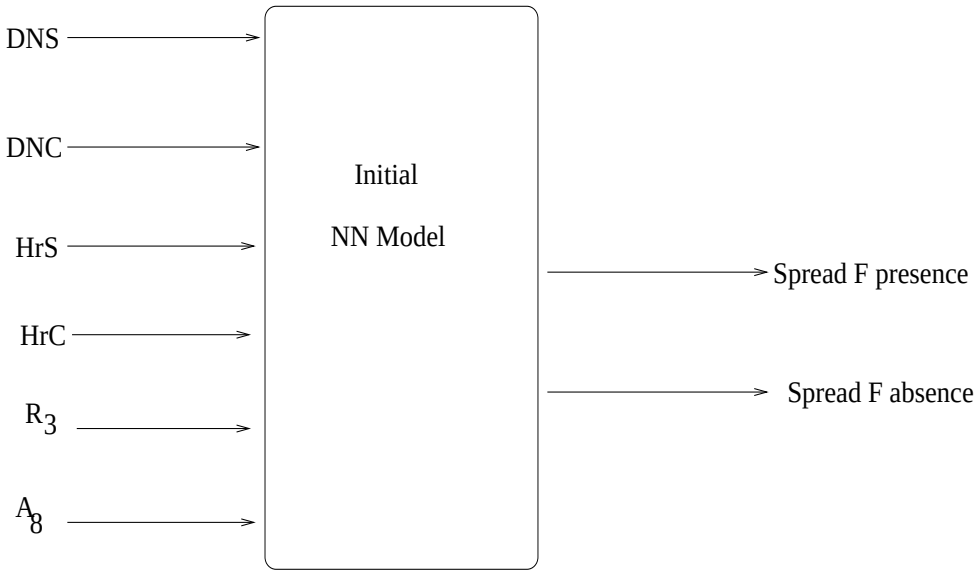

Figure 4.4: Initial NN model for Fortaleza station.

Figure 4.4 shows a block diagram for the NN architecture of the initial model. The same NN architecture and input space is used to develop the Fortaleza and Cachoeira Paulista single station models described later in this chapter.

4.1.7 Initial NN model results

This section presents the initial NN model results. All results could not be presented but those covering the specific days of interest are presented, these include the equinox and solstice days for the periods of high and low solar activity as well as from a period of the dataset not used in training the NNs.

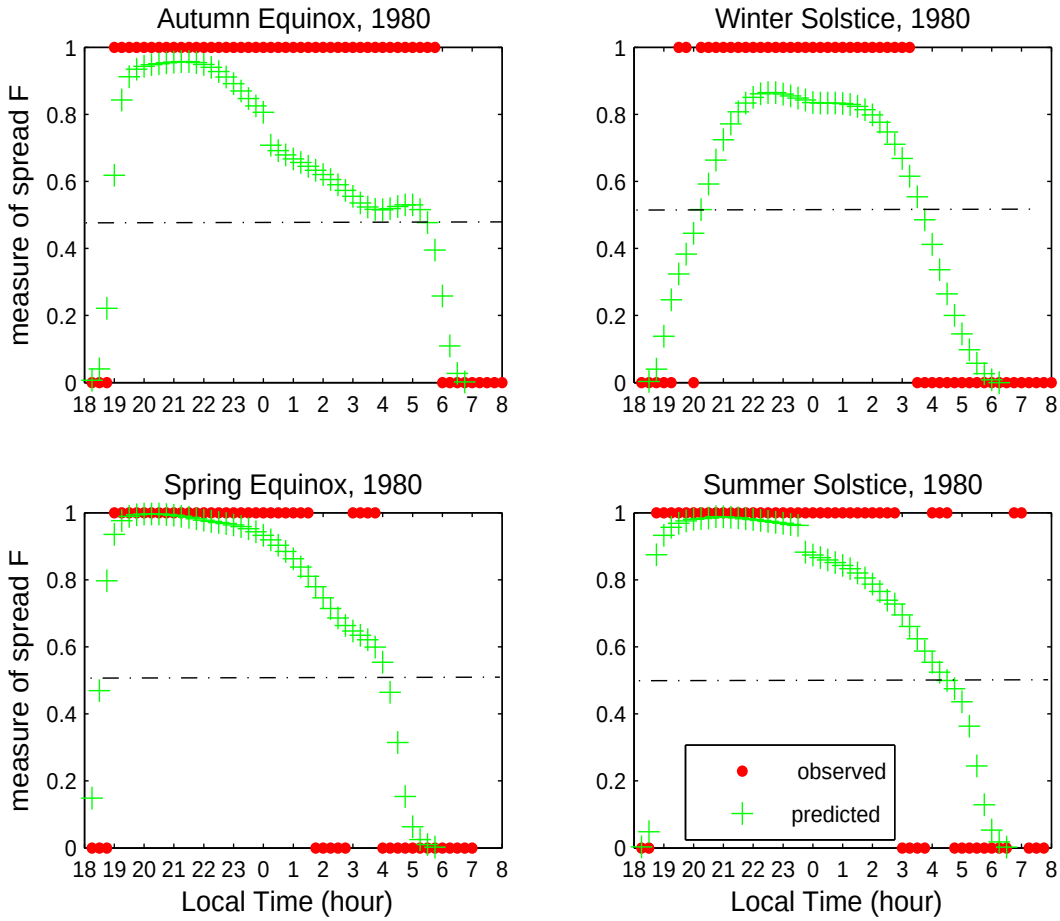

Figure 4.5: First results for Fortaleza during 1980. Both observed (red dots) and predicted (green + signs) measure of spread F are presented.

Figure 4.5 shows the measure of spread F versus local time for Fortaleza during 1980 (near solar maximum). The dotted line indicates a measure equal to 0.5. The NN will always provide a value between 0 and 1, which is inferred as the measure of occurrence of spread F. For the NN models presented in this thesis a measure greater than 0.5 for spread F presence indicates the occurrence of spread F. Taking this into account and looking at the results presented in figure 4.5 it can be seen that the NN results are in good agreement with the observed measure of spread F. The results show that spread F occurs mostly during the night to early morning hours.

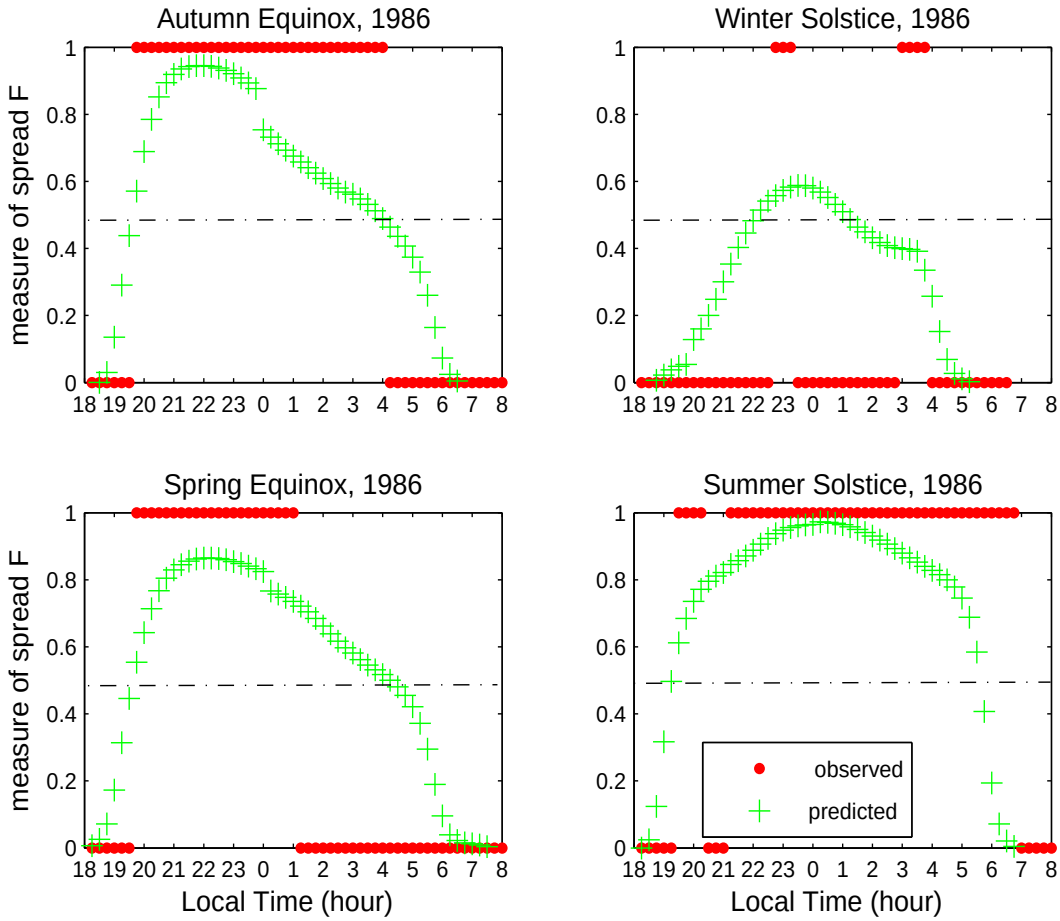

Figure 4.6: Results for Fortaleza during 1986; both observed (red dots) and predicted (green + signs) measure of spread F are presented.

Figure 4.6 shows the predicted and observed measure of spread F versus local time for the equinox and solstice days during solar minimum. It can be deduced that during the winter sostice there is an isolated occurrence of spread F. For the winter solstice, the predicted measure of spread F is less than 0.5 indicating an absence of spread F and this is in agreement with the observed measure of spread F. Figures 4.5 and 4.6 show that a NN can reproduce the patterns learnt, since the data for 1980 and 1986 represented in these figures were used during training.

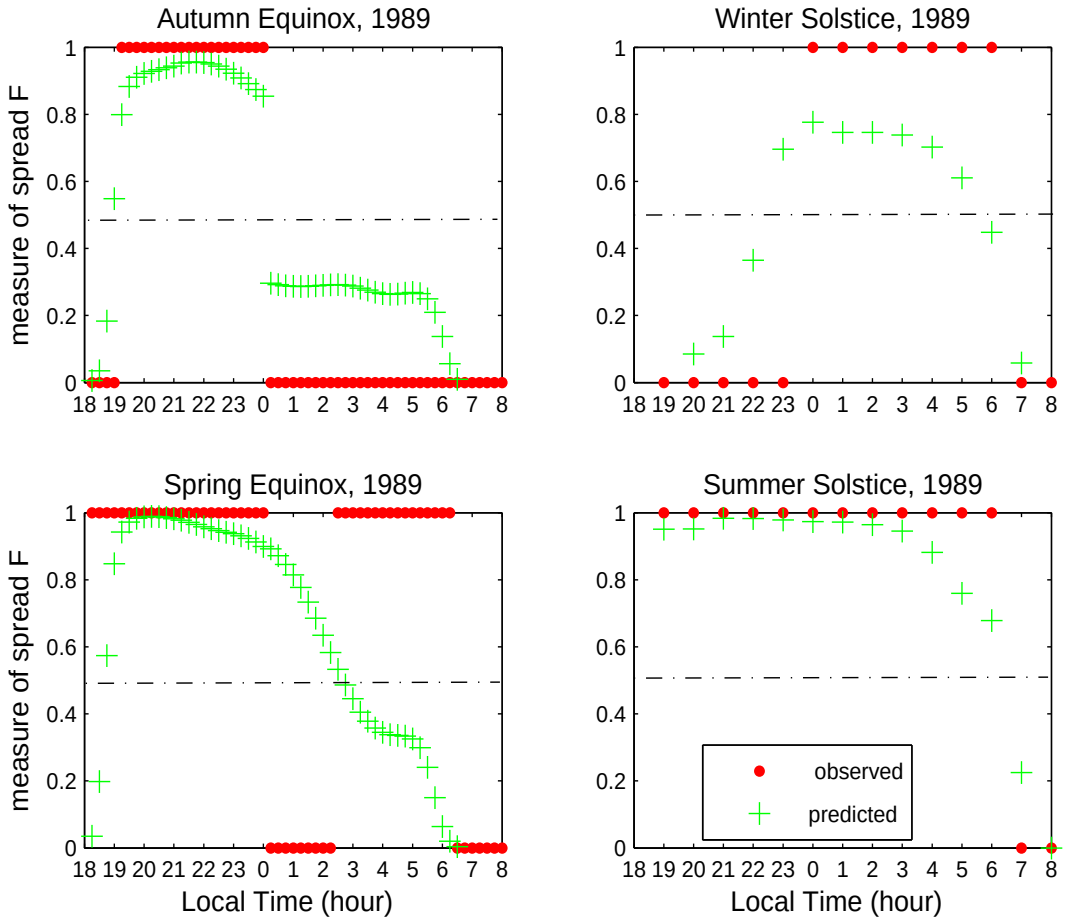

Figure 4.7: Results for Fortaleza during 1989; both observed (red dots) and predicted (green + signs) measure of spread F are presented.

Figure 4.7 shows the measure of spread F versus time for Fortaleza for 1989, a period which was not used as part of the NN training. The predominant feature of a low measure of spread F during the winter solstice is also evident. For the spring equinox, there is a midnight absence of spread F.

4.2 Frequency and range spread F occurrence statistics

There are different mechanisms giving rise to frequency and range spread F, hence there is a need to separate the two when investigating spread F occurrence at different stations (i.e to study the latitudinal dependence of spread F occurrence). Furthermore, considering only range spread F will not affect the NN architecture since the occurrence of frequency spread F in the dataset used in this study is far less than the occurrence of range spread F.

A comparison of range and frequency spread F probability of occurrence is shown in Figures 4.8 and 4.9 for Fortaleza and Cachoeira Paulista stations respectively. The yearly probability of spread F was calculated as the ratio of the sum of the measure of spread F to the total number of observations made during the year (i.e the number of times spread F occurred to the number of observations made) expressed as a percentage by

$$\frac{Sum\ of\ spread\ F\ occurrences}{Total\ number\ of\ possible\ observations} \times 100\% \tag{4.4}$$

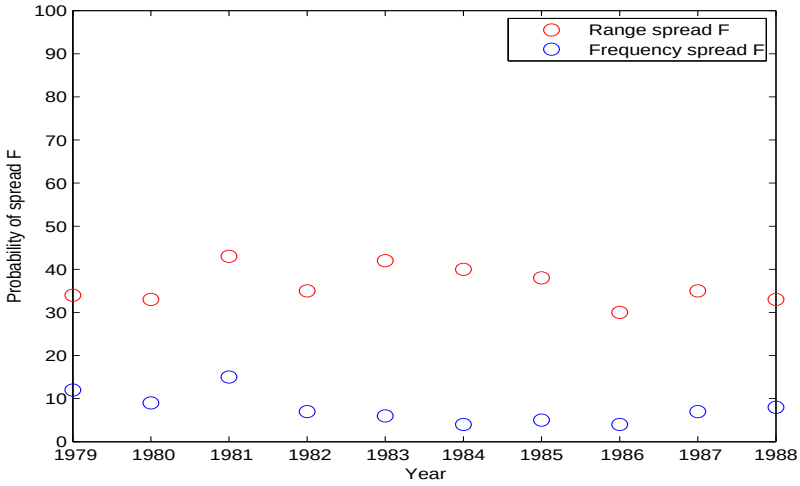

Figure 4.8: A comparison of the probability of range and frequency spread F for Fortaleza station expressed as a percentage for each year of the data used in training is presented.

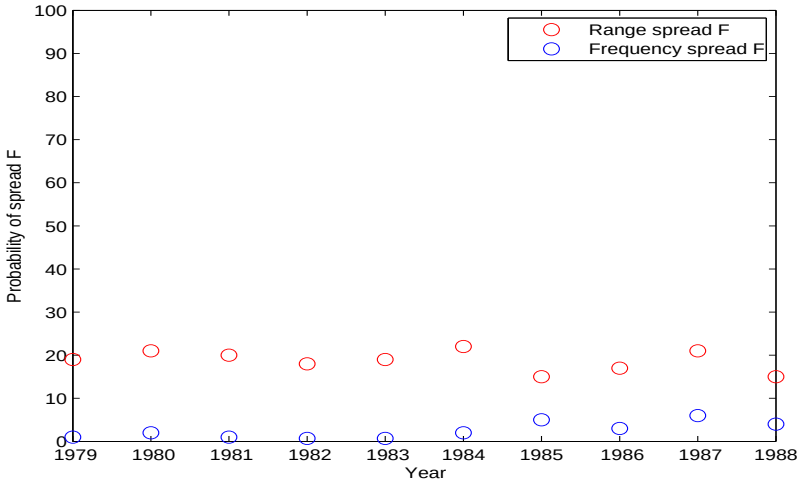

Figure 4.9: A comparison of the probability of range and frequency spread F for Cachoeira Paulista station expressed as a percentage for each year of the data used in training is presented.

Figures 4.8 and 4.9 show that in general range spread F occurs more frequently than frequency spread F for both stations given the data available. Thus, for selected stations, the occurrence of frequency spread F is insignificant and may not have significantly contributed to the resulting initial model

architecture. Only range spread F data was therefore used to develop the Fortaleza and Cachoeira Paulista single station models.

4.3 Fortaleza station NN model (FSNN)

The input parameters consisted of seasonal (DNC & DNS), diurnal (HrC & HrS), Ap index (dairly running mean, A_8) and sunspot number (three-month running mean, R_3). These inputs are the same as the ones for the initial model except that only range spread F data was considered for the output parameters.

The FSNN model was trained with data corresponding to a full sunspot cycle (from 1978 to 1988 inclusively) from Fortaleza station (3.9°S, 38.45°W, dip angle: -9°). The FSNN model was tested using the entire dataset used in training and an RMSE value of 0.3494 was obtained which is an improvement over the RMSE value of 0.3605 obtained for the initial NN model.

The probability of spread F was calculated using:

$$\frac{Sum\ of\ spread\ F\ occurrences}{Total\ number\ of\ possible\ observations} \times 100\% \tag{4.5}$$

for each month expressed as a percentage. The results from the FSNN model are presented in Figure 4.10.

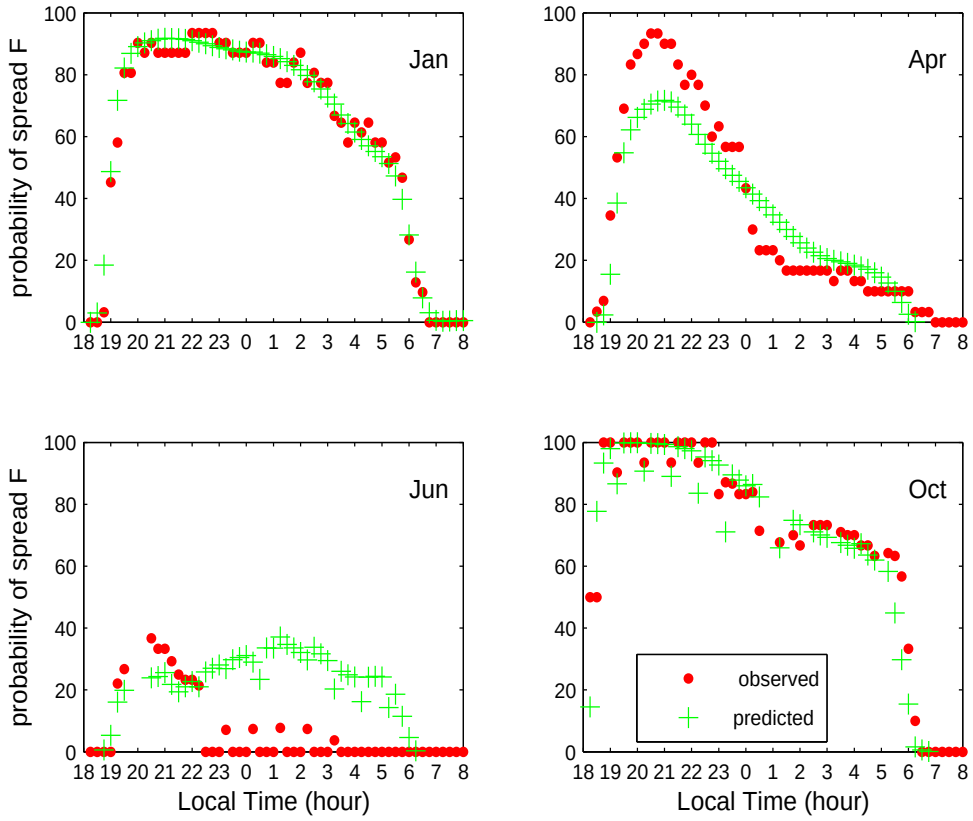

Figure 4.10: Results for Fortaleza station NN model showing the probability of spread F in monthly percentage versus local time for January, April, June and October of 1989.

Figure 4.10 shows the probability of spread F versus local time for selected months in 1989 for Fortaleza station. The data for 1989 was not used as part of the training set, hence these results can be taken as a performance test for the Fortaleza station NN model. The results from the FSNN model are in good agreement with the observed probabilities. In June, however, the FSNN gives higher probabilities in the early morning hours and lower probabilities during late evening in April. Inasmuch as this is a higher prediction, it is still very low (averaging around 30%) and this suggests that the probability of spread F presence is low, this is in good agreement with the observed probability which in this case is a zero probability.

The observed measure of spread F is represented by either ones or zeros (i.e. discrete values) and the NN model always gives a measure between one and zero, thus any predicted measure of spread F close to zero implies no spread F. For this part of my work, no particular attention was paid to the equinox and solstice months for testing results. The results presented here only serve as an illustration that a NN can be used to predict the measure of occurrence of spread F. However, chapter 5 presents the results for these periods.

4.4 Cachoeira Paulista Station NN model (CPNN)

As with the FSNN, the input parameters consisted of seasonal (DNC & DNS), diurnal (HrC & HrS), Ap index (dairly running mean, A_8) and sunspot number (three-month running mean, R_3). Only range spread F data was used for the output parameters. The CPNN model was trained with data corresponding to a full sunspot cycle (from 1978 to 1988 inclusively) from Cachoeira Paulista station (22.6°S, 45°W, dip angle: -28°). The results from the CPNN model are presented in Figure 4.11.

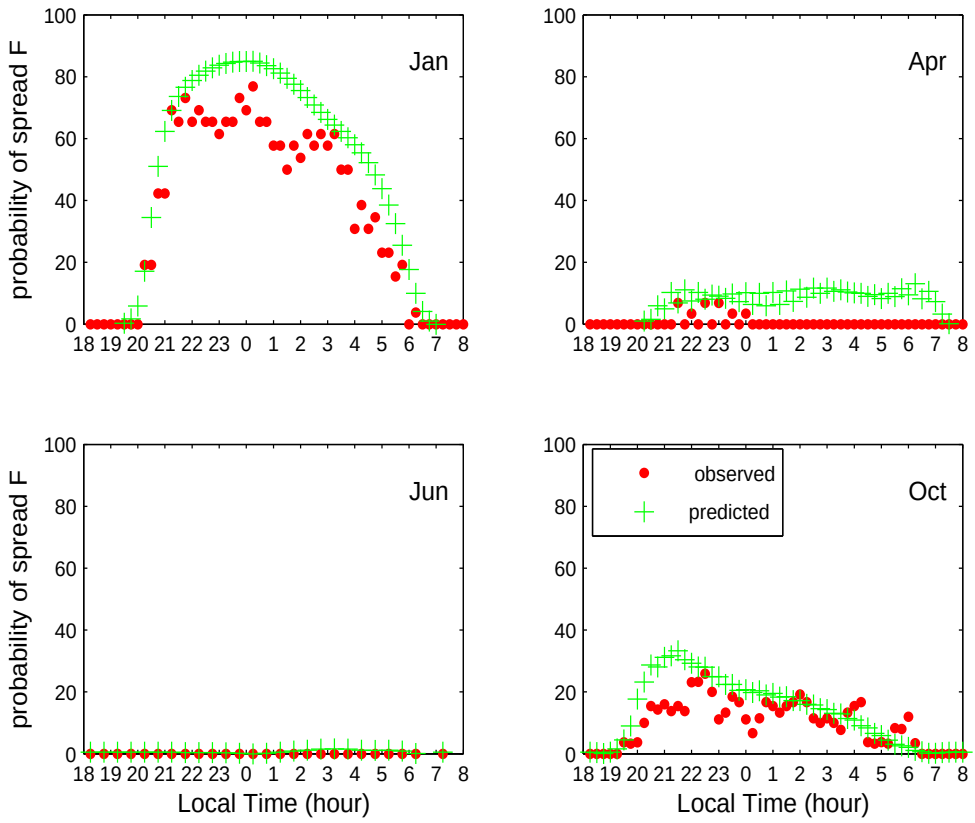

Figure 4.11: Results for Cachoeira Paulista station NN model showing the probability of spread F in monthly percentage versus local time for January, April, June and October of 1989

Figure 4.11 shows the probability of spread F versus local time for selected months in 1989 for Cachoeira Paulista station. The data for 1989 was not used as part of the training set, hence these results can be taken as a performance test for the Cachoeira Paulista station NN model. The results from the CPNN model are in relatively good agreement with the observed probabilities.

4.5 Summary of results

An interpretation of spread F data has been given and the development of an initial single station model has been presented. The resulting initial single

station model results can be summarised as follows:

- The measure of occurrence of spread F can be predicted using a model developed with the technique of NNs.
- NN results show the onset and peak occurrence of spread F.
- Spread F is a night-time phenomenon at the equatorial and low latitudes.
- The initial NN model can be summarised as follows:

$$f\left(DNC, DNS, HrC, HrS, A_8, R_3\right) = measure\ of\ spread\ F \tag{4.6}$$

The yearly probability of frequency spread F is low, averaging below 10% at Fortaleza station and below 5% at Cachoeira Paulista station. This indicates that at the equatorial and low latitude regions, range spread F is more predominant in comparison to frequency spread F. As such, to gain an insight into spread F occurrence at the equatorial and low latitude regions, it is advisable to consider range spread F.

Following the development of the initial NN model, the single station models were developed and the results of the single station models can be summarised as follows:

Both FSNN and CPNN models perform acceptibly in predicting the measure of occurrence of spread F. The FSNN model results show a peak occurrence of spread F in January and October (corresponding to summer and spring months) with the occurrence during the night-time to early morning hours. The FSNN results show a post-sunset peak occurrence in spread F activity in April (autumn) and a low occurrence during early morning hours. In addition, the FSNN model shows less likelihood of occurrence of spread F during the post-sunset and early morning hours in June (winter) for Fortaleza station than in other seasons.

The CPNN model results show a peak in the probability of spread F in January, and a less likelihood of spread F in April, June and September (corresponding to autumn, winter and spring respectively).

A closer look at the FSNN and CPNN model results show a delay in spread F peak occurrence in January at Cachoeira Paulista station as compared to Fortaleza station, i.e. there is a peak occurrence around 19:00 LT to about 03:00 LT at Fortaleza station and a peak occurrence around 21:00 LT to about 01:00 LT at Cachoeira Paulista station.

The two single station model results show that on average there is more spread F activity at Fortaleza (equatorial latitude) than at Cachoeira Paulista (low latitude).

Chapter 5

Brazilian sector spread F models

5.1 Introduction

This chapter outlines the development of the Brazilian sector NN model (BSNN). The BSNN model was used to make predictions for 1985 and 1989. The BSNN model results are presented and discussed in a way that shows the diurnal, seasonal and latitudinal variability of the occurrence of spread F. An analysis of errors was performed together with a comparison of the BSNN and Abdu (Abdu *et al.*, 2003) models.

5.2 Brazilian sector NN model

Range spread F data from two Brazilian stations, Fortaleza (equatorial latitude, 3.9°S, 38.45°W) and Cachoeira Paulista (low latitude, 22.6°S, 45°W) were used in the development of the BSNN model. Figure 5.1 shows the relative geographic positions of these two stations.

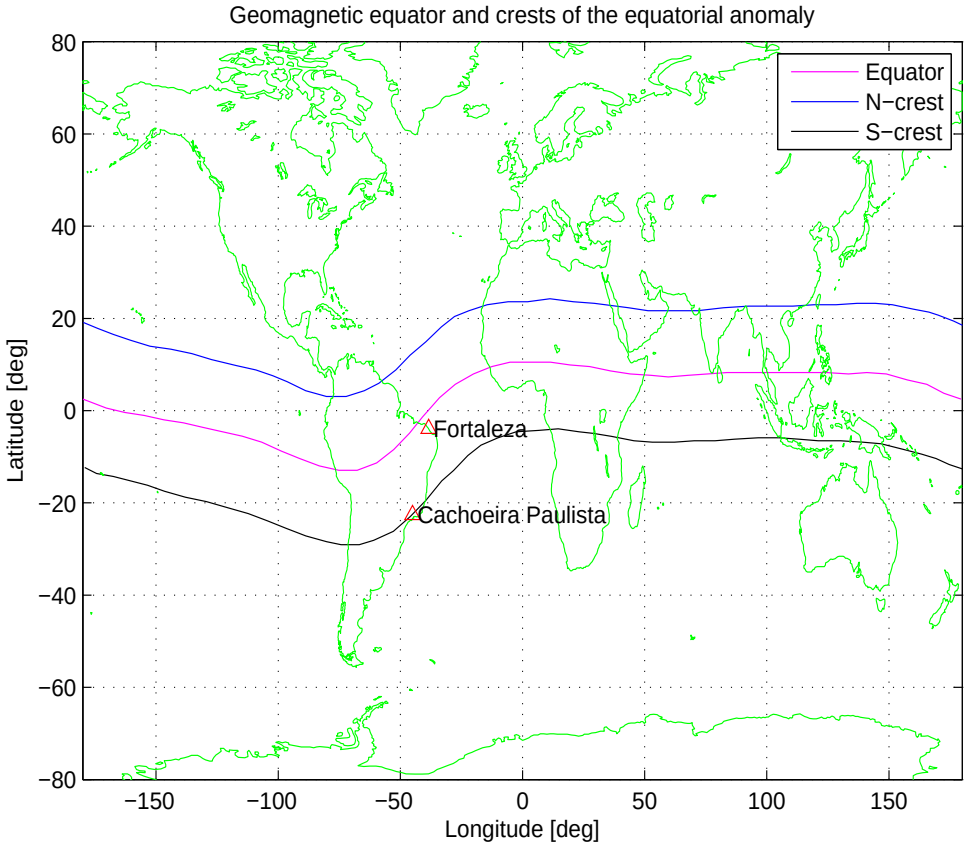

Figure 5.1: Map showing the geographic locations of Fortaleza and Cachoeira Paulista in Brazil.

5.2.1 Magnetic latitude and colatitude

The magnetic colatitude θ is defined as the angular distance along a magnetic meridian from a point of observation to the north magnetic pole. The magnetic equator is the great circle with a magnetic colatitude equal to 90°. The magnetic latitude λ is the angular distance from the magnetic equator in the direction of the north/south magnetic pole to the point of observation (Cox and Hart, 1996). These two are related via:

$$\lambda = 90 - \theta \tag{5.1}$$

The relationship between the magnetic colatitude and magnetic inclination (I) is given by

$$tan(I) = 2cot(\theta) \tag{5.2}$$

This reduces to

$$tan(I) = 2tan(90 - \theta) \tag{5.3}$$

Therefore

$$tan(I) = 2tan(\lambda) \tag{5.4}$$

5.2.2 The BSNN model inputs

The development of the BSNN model is based upon the known variability of the occurrence of spread F. The variability can be classified as long term (sunspot cycle controlled), medium term (seasonal), short term (diurnal) and irregular (controlled by dynamic parameters including but not limited to magnetic activity, thermospheric winds and F2 layer height). Latitudinal variability is another factor that is considered when developing a regional model. The BSNN model was developed using the same NN architecture and input space as the FSNN and CPNN models: the only difference was the inclusion of station information for the BSNN model.

The following parameters were used as inputs to the BSNN model:- geographic latitude (lat), magnetic declination (dec) and inclination (inc), seasonal (DNS and DNC), diurnal (HrS and HrC), magnetic activity (A_8, a running mean of the previous eight 3-hourly Ap index values) and solar activity (R_3, a three-month running mean of the sunspot number). The magnetic latitude of a station is a very important parameter in determining the occurrence of spread F since it is related to the magnetic inclination of that particular geographic position. An occurrence of spread F, represented by spread F presence and spread F absence, were the outputs to the BSNN model. The BSNN model produces the function F such that

$$P = F(lat, dec, inc, DNS, DNC, HrC, HrS, A_8, R_3) \tag{5.5}$$

Where P refers to the measure of occurrence of spread F.

The magnetic declination and inclination data was obtained from the website (http://www.ngdc.noaa.gov/geomagmodels/IGRFWMM.jsp) while the sunspot and Ap index data was obtained from (http://spidr.ngdc.noaa.gov/spidr/index.jsp). The resulting BSNN model is shown in Figure 5.2.

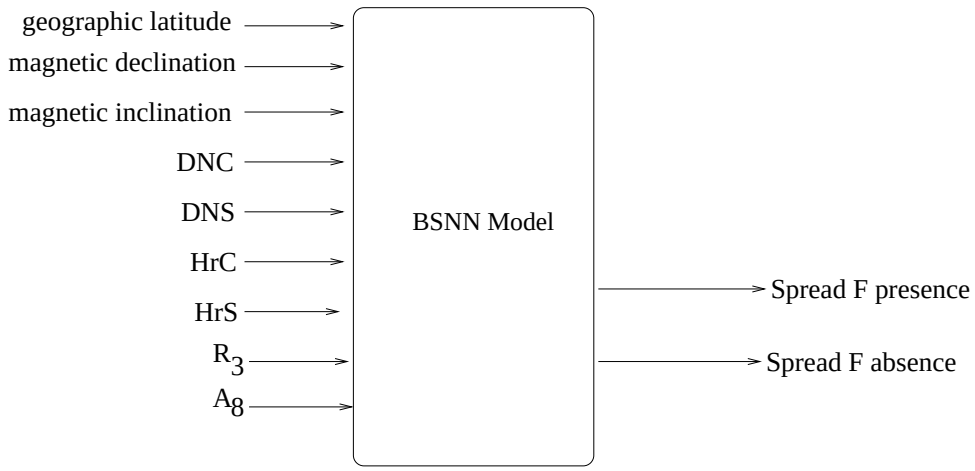

Figure 5.2: The Brazilian sector NN model (BSNN), showing the input and output parameters.

5.3 The BSNN model results

The BSNN model was trained using range spread F data (from 1978 to 1988 inclusively) from Cachoeira Paulista and Fortaleza in Brazil. The resulting BSNN model was used to predict the occurrence of spread F for the two stations for the years 1985 and 1989. Data for the year 1985 was used in training the network. However, since there was no data available that corresponded to a period of solar minimum outside the data range used during training, the year 1985 was used to determine the performance of the BSNN model during a period of low solar activity. Data for 1989 was not used as part of the training dataset, which means that the results presented for this year serve as an application of the BSNN model to unseen data, and indicate the model's ability to generalise the output.

The results from the BSNN model were arranged into monthly bins with each bin containing the occurrence of spread F as a function of local time. The probability of spread F was calculated in monthly percentage by

$$\frac{Sum\ of\ spread\ F\ occurrences}{Total\ number\ of\ possible\ observations} \times 100\% \tag{5.6}$$

The reason for dealing with the probability of spread F in monthly percentage is that this provided monthly trends in spread F occurrence. The present literature has dealt extensively with monthly trends in spread F occurrence statistics, this therefore means that a starting point in modelling or predicting spread F occurrence should agree with the already existing models designed for the same purpose.

The probability of spread F as a function of local time and latitude and arranged according to season expressed as a percentage is presented in figures 5.3 - 5.10. In these figures, the red coloured dots represents the probability of spread F as observed on ionograms (measured data) while the green coloured plus signs represents the probability of spread F presence as predicted by the BSNN model.

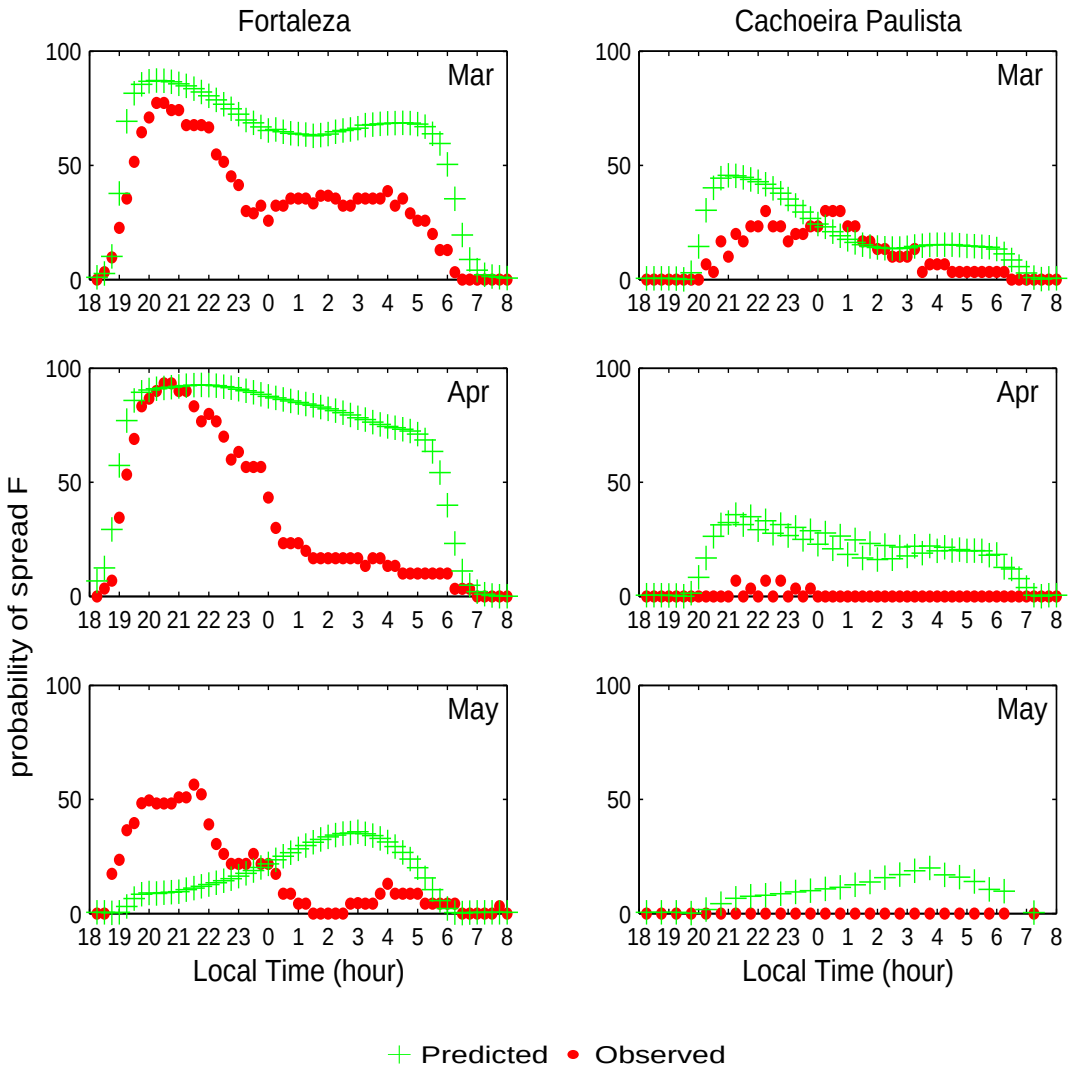

Figure 5.3: A comparison of observed (red dots) and predicted (green plus signs) probability of spread F for the Brazilian sector for autumn of 1989 (high solar activity) expressed as a percentage.

The results are presented in a form that allows for a comparison of the BSNN model and the observed data. The best way to study the trends in the probability of spread F is to look at the peak probability, peak onset and offset times, and the duration of the peak. One can then define a period of high spread F activity as a period with a high probability and a long duration of spread F above a given threshold of probability. We can also define a moder-

ate activity as a period with relatively high peak probability and a moderate duration of spread F above a given threshold of probability. A period of low spread F activity will be defined by a low peak percentage occurrence and a short duration of spread F occurrence above a given threshold of probability. For the purpose of this study, a 50% threshold probability will be considered to favour the probability of spread F presence.

Figure 5.3 presents the results during the autumn of 1989. The BSNN model predictions are in agreement with the observed probabilities during the nighttime period from 18:00 LT to 23:00 LT for the latitudes of Fortaleza and Cochoeira Paulista. However, during the early morning hours, the BSNN model overpredicts the observed probabilities at Fortaleza.

In May at Fortaleza, the BSNN model predicts the night-time probabilities to be lower than the observed ones and the early morning probabilities higher than the observed ones. All the predicted probabilities are less than 50% and therefore there is less likelihood of spread F presence in May at the equatorial site Fortaleza than there is of spread F absence, i.e. there is a 50% plus likelihood of spread F absence. A decrease in spread F likelihood is observed as autumn progresses. This decrease is more pronounced at Fortaleza. In general the results show that Cachoeira Paulista has a lower spread F activity during the autumn months than Fortaleza.

Figure 5.4 presents the results for winter in 1989. For June and July at Fortaleza, the BSNN model predicts the spread F probabilities to be higher than the observed probability of spread F during the early morning hours. During June and July there was almost no spread F at Cachoeira Paulista during the early morning hours. From the observed data it can be seen that at both Fortaleza and Cochoeira Paulista there is a low probability of occurrence of spread F after midnight during June and July. For Cachoeira Paulista station, the BSNN model gives predictions that are within 20% of the observed probabilities. The results also show an increase in the predicted probability of spread F activity as the winter progresses at Fortaleza, which

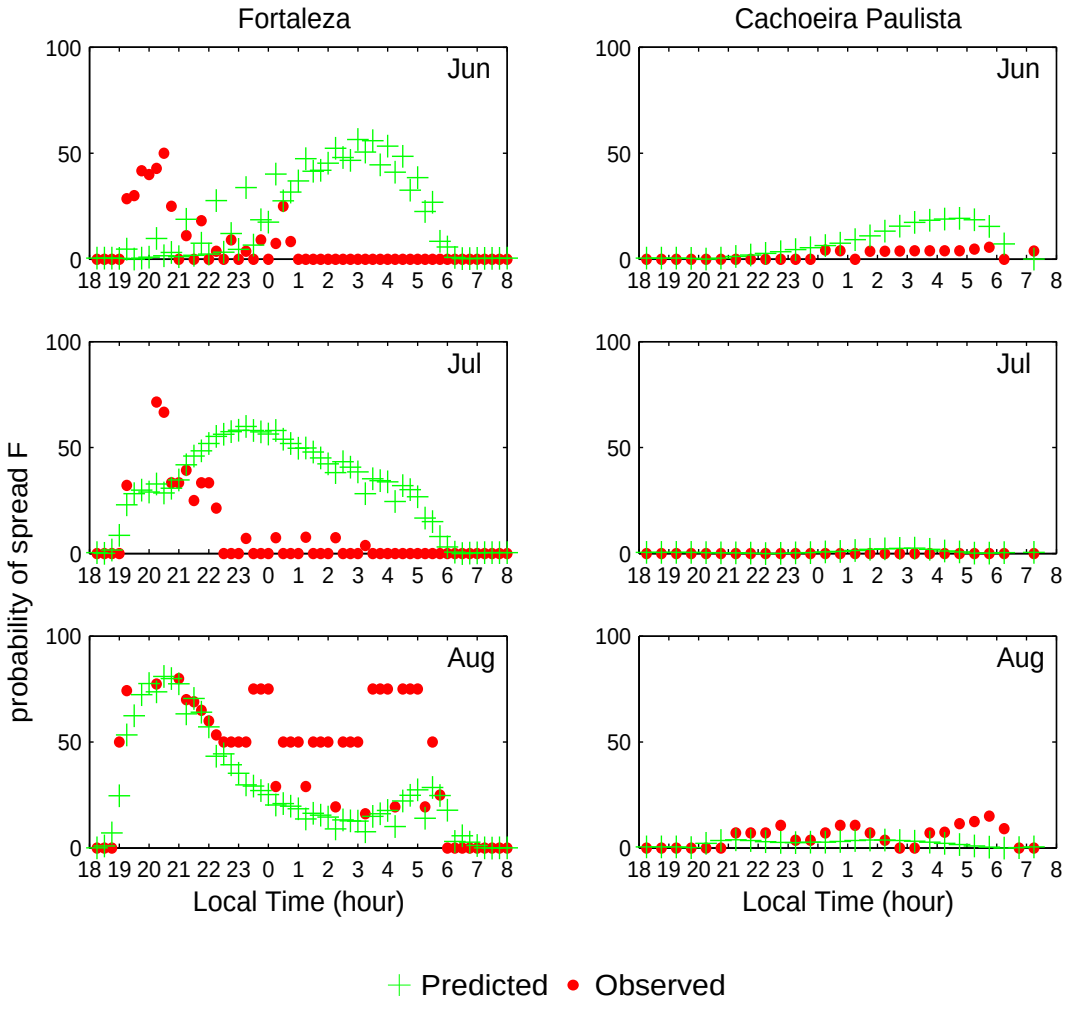

Figure 5.4: A comparison of observed (red dots) and predicted (green plus signs) probability of spread F for the Brazilian sector for winter of 1989 (high solar activity) expressed as a percentage.

is closer to the equator, with August having a peak percentage occurrence around 19:00 LT to 23:00 LT with less likelihood of occurrence during the early morning hours. The BSNN model predicted a low average occurrence of spread F in the early morning hours in August at Fortaleza. This is because the NN is good at generalising the solution rather than being too specific. In this case, however, the BSNN model has gone with the average low spread F occurrence during the early morning hours.

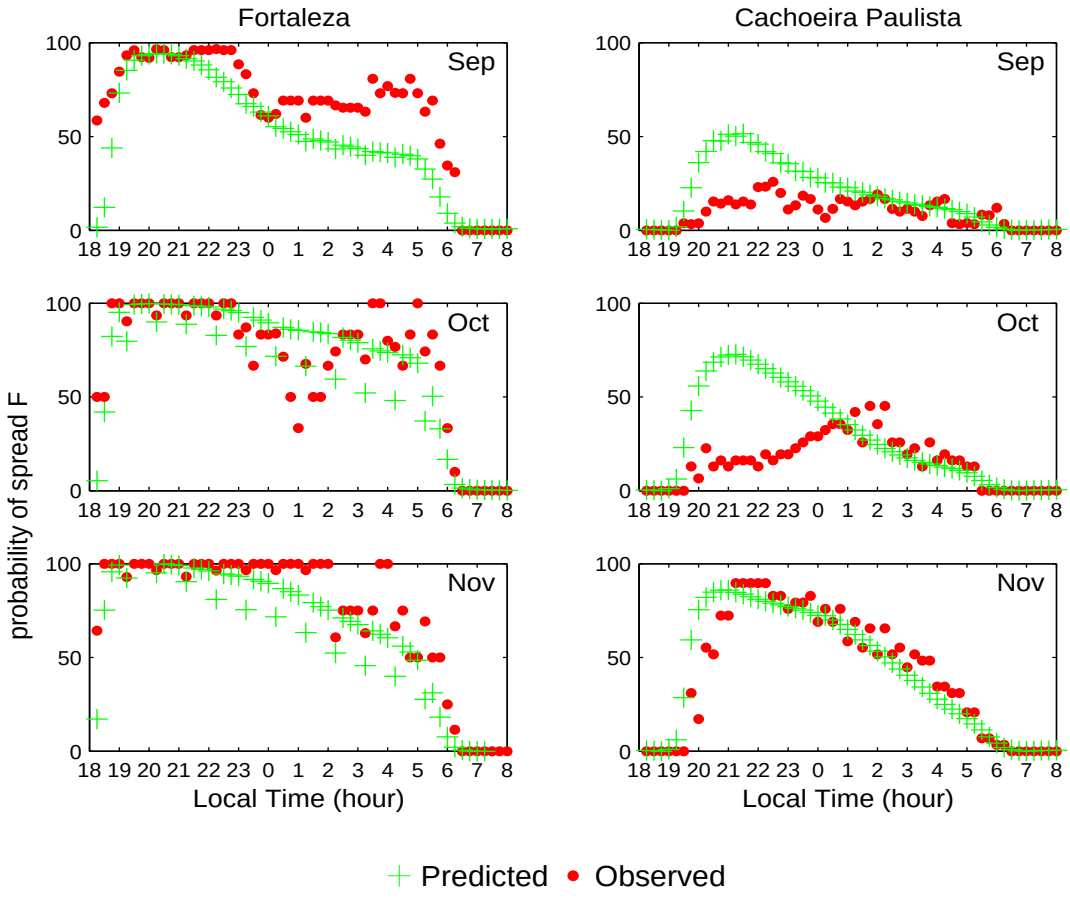

Figure 5.5: A comparison of observed (red dots) and predicted (green plus signs) probability of spread F for the Brazilian sector for spring of 1989 (high solar activity) expressed as a percentage.

Figure 5.5 presents the results for spring in 1989. In October at Cachoeira Paulista, the BSNN model predicted the early evening spread F probabilities to be higher than the observed ones. However, the early morning BSNN model spread F probabilities are closer to the observed probabilities. The other predicted results for spring of 1989 are within 25% of the observed probabilities. Spread F activity increases at both stations as the spring progresses. However, there is still less spread F activity at Cachoeira Paulista than Fortaleza.

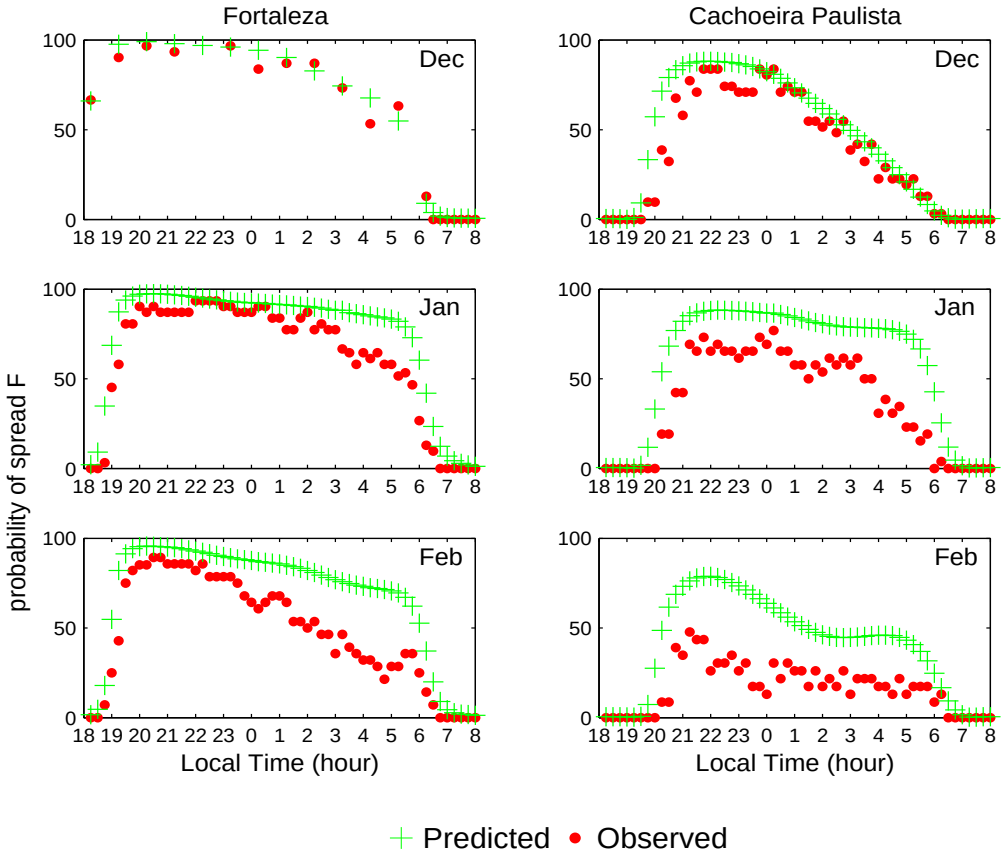

Figure 5.6: A comparison of observed (red dots) and predicted (green plus signs) probability of spread F for the Brazilian sector for the summer of 1989 (high solar activity) expressed as a percentage.

Figure 5.6 presents the results for the summer of 1989. In February at Cachoeira Paulista, the BSNN overpredicts the probabilities of spread F occurrences for all hours when spread F was present. However, the general trend of the spread F probability rising to a peak in the evening and decreasing towards dawn is predicted by the model. For the rest of the summer the predicted probabilities are within 30% of the observed ones. The results for summer of 1989 indicate a higher spread F activity at both latitudes than during the other seasons.

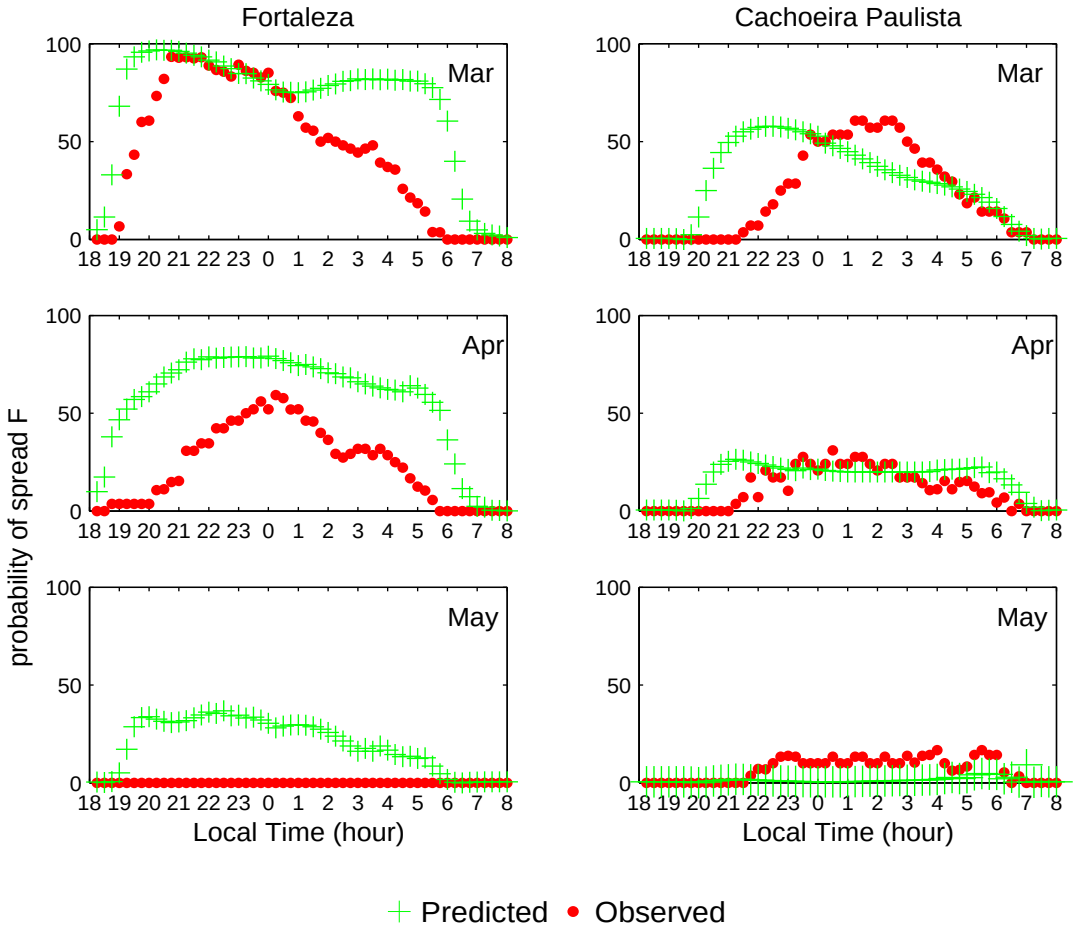

Figure 5.7: A comparison of observed (red dots) and predicted (green plus signs) probability of spread F for the Brazilian sector for autumn of 1985 (low solar activity) expressed as a percentage.

Figure 5.7 shows the results during the autumn of 1985, a period of low solar activity (near to the minimum of the solar cycle). The BSNN model predicted an early peak probability of spread F occurrence at the low latitude site of Cachoeira Paulista with peak occurrence at about 22:00 LT while the observed data indicates a peak around local midnight hours in March. In May at Fortaleza, the BSNN model predicted probabilities that are higher than observed, however, the predicted probabilities are not high enough to suggest an occurrence of spread F.

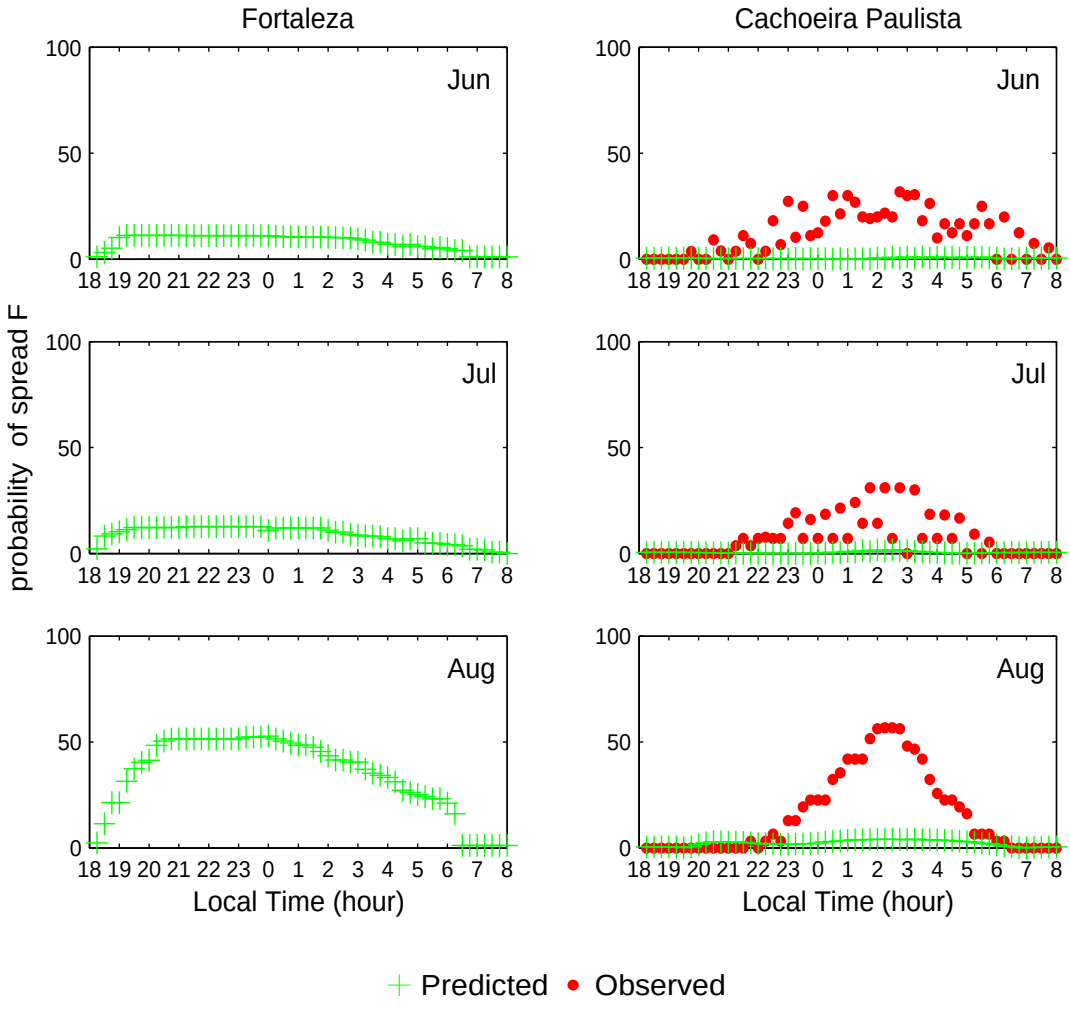

Figure 5.8: A comparison of observed (red dots) and predicted (green plus signs) probability of spread F for the Brazilian sector for the winter of 1985 (low solar activity) expressed as a percentage.

Figure 5.8 presents the results for the winter of 1989. There were no data for Fortaleza during the winter months. At Cachoeira Paulista, the BSNN predicts an absence of spread F for all three months of winter, while there was some activity during the early morning hours every month, with the observed activity increasing in August. The BSNN model results at Fortaleza shows that we can learn something about spread F even if no observed data was available.

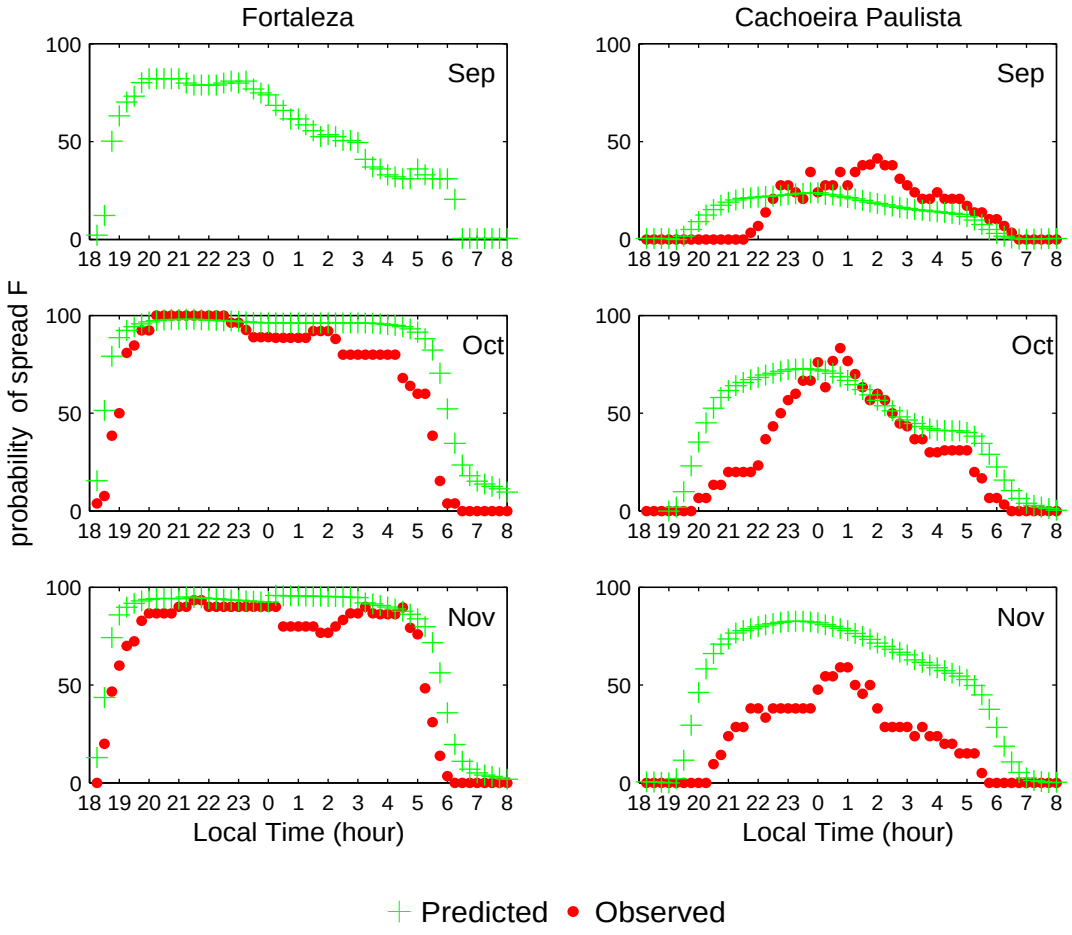

Figure 5.9: A comparison of observed (red dots) and predicted (green plus signs) probability of spread F for the Brazilian sector for spring of 1985 (low solar activity) expressed as a percentage.

Figure 5.9 presents the results for spring of 1985. September data for Fortaleza was not available. The BSNN model performs very well in making predictions except in November at Cachoeira Paulista where the predicted probabilities exceed the observed by an average of 30%. However, these November results are not far off the observed data. The results also show a higher spread F activity at Fortaleza than at Cachoeira Paulista during spring.

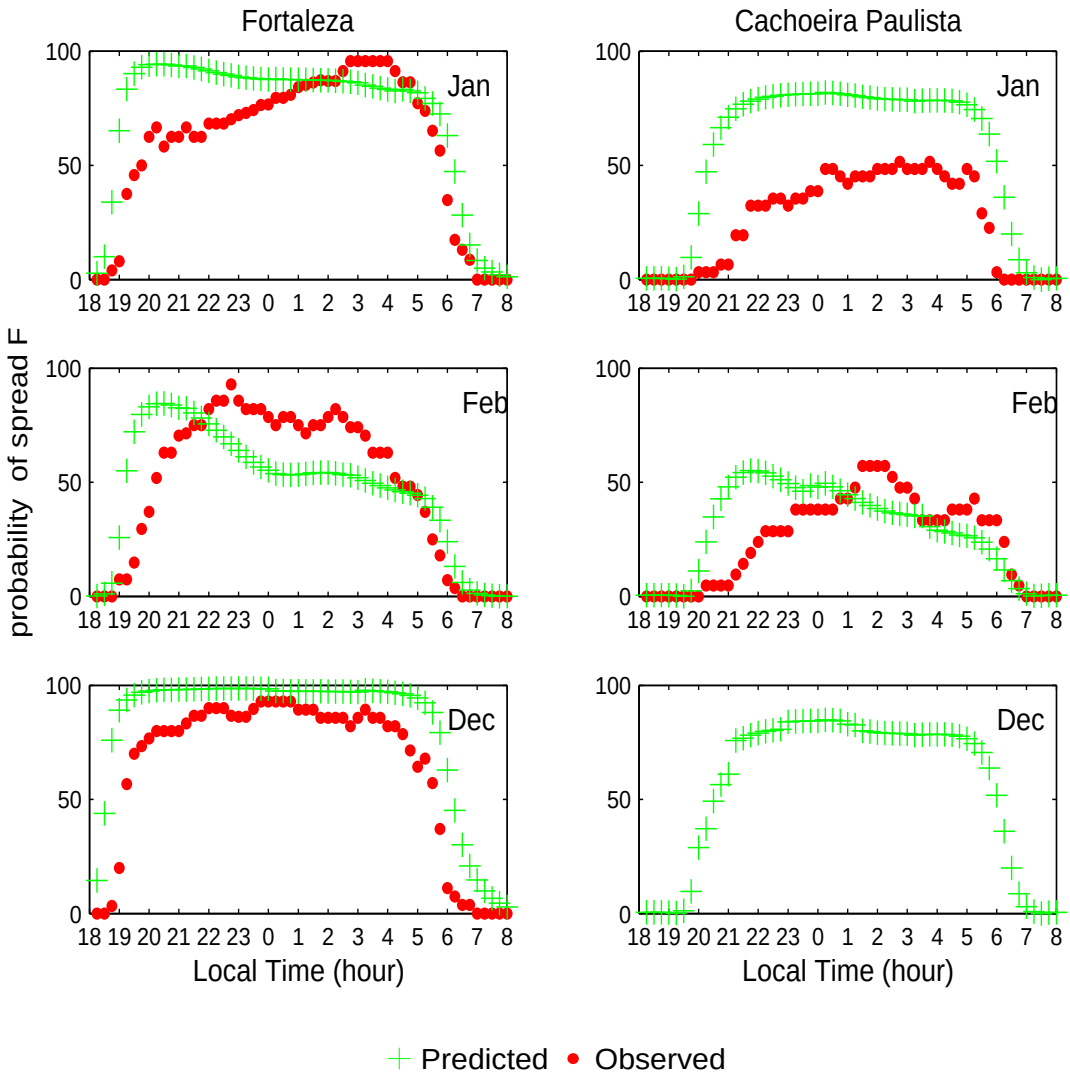

Figure 5.10: A comparison of observed (red dots) and predicted (green plus signs) probability of spread F for the Brazilian sector for the summer of 1985 (low solar activity) expressed as a percentage.

Figure 5.10 gives the results for the summer months of 1985. No data was available for Cachoeira Paulista for December. The BSNN model results are within 20% of the observed data in all cases except January at Cachoeira Paulista, where the BSNN model predicted probabilities 40% above the observed probabilities. There was a higher spread F activity at Fortaleza in the evening in December 1985 than there was in January of the same year. In

general the BSNN model correctly predicted the common observed trends of the probability of spread F at the low latitude site Cachoeira Paulista more accurately than at the equatorial site Fortaleza during the summer months of a year near the solar cycle minimum.

5.3.1 Consistency Check

The BSNN model has two outputs, these outputs indicates a measure of occurrence of spread F (absence or presence). The graphs in figures 5.3 to 5.10 only represent spread F presence. Figure 5.4 shows that the BSNN model predicts an absence of spread F in July at Cachoeira Paulista.

Figure 5.6 shows that the BSNN model predicts an occurrence of spread F in January at Fortaleza. As a consistency check, Figure 5.11 shows the probability of spread F absence for January at Fortaleza and July at Cachoeira Paulista.

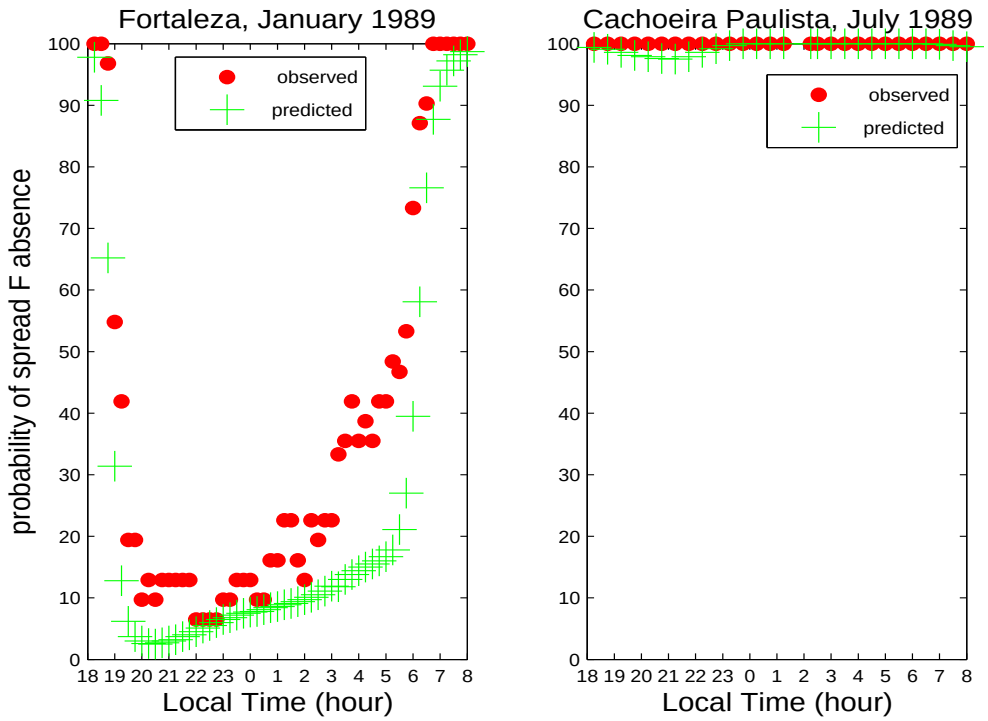

Figure 5.11: A comparison of observed (red dots) and predicted (green plus signs) probability of spread F absence for January at Fortaleza and July 1989 at Cachoeira Paulista.

These results show the occurrence of spread F in January at Fortaleza and no spread F occurrence in July at Cachoeira Paulista. The BSNN model correctly predicts spread F presence in January at Fortaleza and no spread F occurrence in July. This section was included for completeness.

5.4 Error Analysis

This section presents an analysis of the accuracy of the BSNN model in terms of the difference between the predicted and observed probabilities. These differences determine the overall performance of the BSNN model. A positive difference indicates that the BSNN model predicts higher than observed probabilities over the same period while a negative difference indicates that the BSNN model predicts lower than the observed prbabilities over the same period.

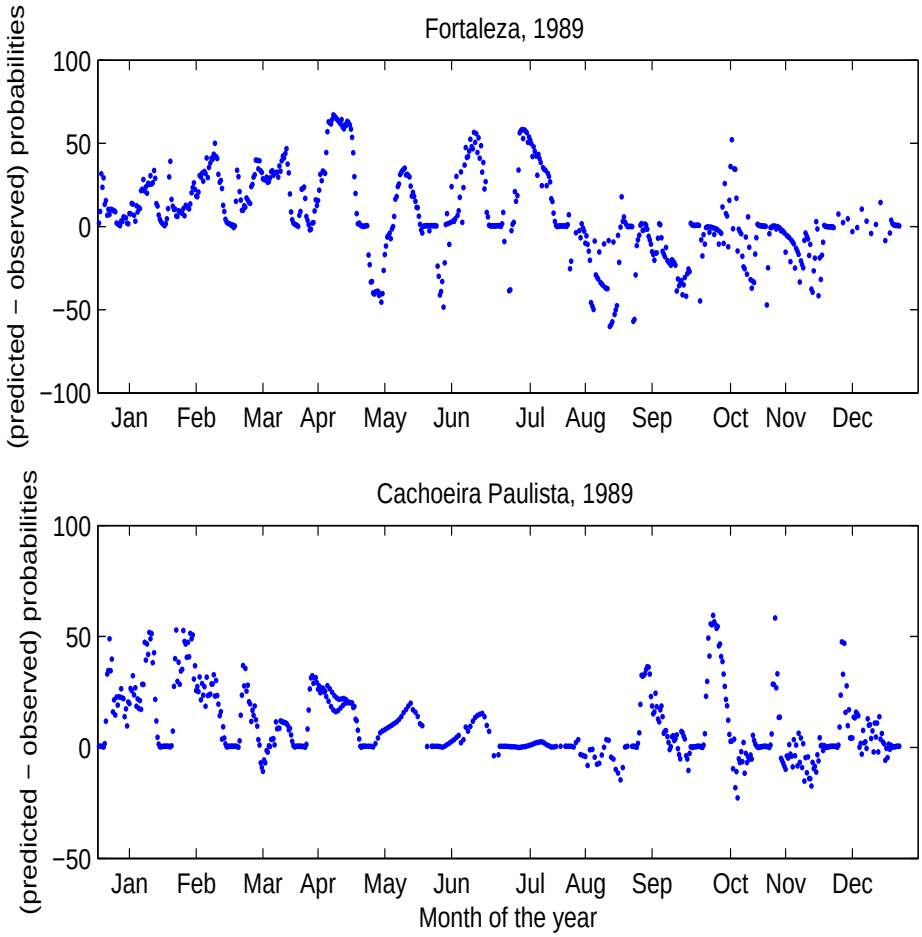

Figure 5.12: The difference between the predicted and the observed probabilities for the BSNN model for 1989 (high solar activity) is shown for Forteleza (top panel) and Cachoeira Paulista (bottom panel).

In Figure 5.12, the differences in the predicted and observed probabilities for both stations are presented for each month for a given local time plotted for night time to morning hours. The sharp peaks at the start and end times result from the fact that the BSNN model slowly migrates from an occurrence close to zero to close to one while the actual data has a sharp transition from zero to one and vice versa. The results presented here are a summary of the previous results in that the differences give an extent to which the BSNN model differs from the observed data.

Excluding the start and end times, the results show that the BSNN model predictions for Fortaleza differ from the observed data by about 30% from September through to the end of March. It also predicts about 50% higher in the early morning hours in April at Fortaleza. In May at Fortaleza, the BSNN model predicts about 50% lower at night and 50% higher in the early morning hours. In June and July, the BSNN models predicts 50% higher than the observed data during the early morning hours at Fortaleza, and 50% lower in August than observed data.

At Cachoeira Paulista, the BSNN model predicts about 50% higher probabilities in the early morning hours in January and at all times in February than the observed data. From April to August the BSNN model predicts up to about 20% higher probabilities than the observed data at all times. The BSNN model predicts up to about 40% in the evening in September and about 50% in the evening in October higher than the observed data.

Therefore, the above results indicate that the BSNN model provides more accurate predictions during the period from September through to April at Fortaleza and during the period from April to August at Cachoeira Paulista in terms of the actual probabilities. However, the predicted trends in onset times, peak occurrence, diurnal variations, seasonal variations and latitudinal variation in spread F are correctly predicted by the BSNN model for all the seasons represented by the results. This is discussed further in the following sections.

5.4.1 Input space analysis

The number of available data points for 1980 (near solar maximum) and 1985 (near solar minimum) corresponding to periods of high and low solar activity for Fortaleza and Cachoeira are presented. The performance of a NN model is dependent on the amount of data available for training that uniformly represents the input space. Therefore, it is necessary to analyse the data available for training the BSNN model before discussing the results.

The monthly mean for the available data was calculated as the mean of all the available 15 minute data points in each month. The procedure involved arranging the data into 15 minute data bins for each month, then determining the total number of data available at each 15 minute interval. Data availability in terms of the number of 15 minute intervals for which data was available was expressed as a percentage of all the 15 minute intervals. A 100% availability means that all the 15 minute data points for a month were available. Figures 5.13 - 5.16 show the availability of data for the two years analysed.

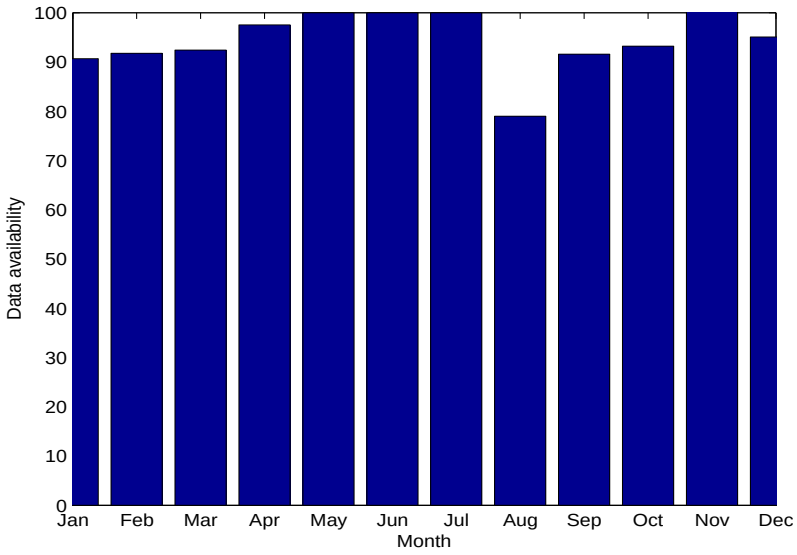

Figure 5.13: A graph showing the availability of training data for Fortaleza in 1980.

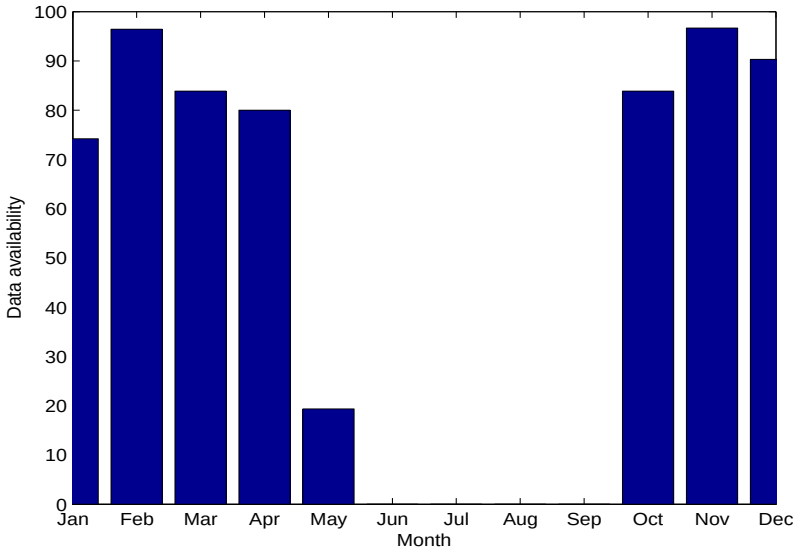

Figure 5.14: A graph showing the availability of training data for Fortaleza in 1985.

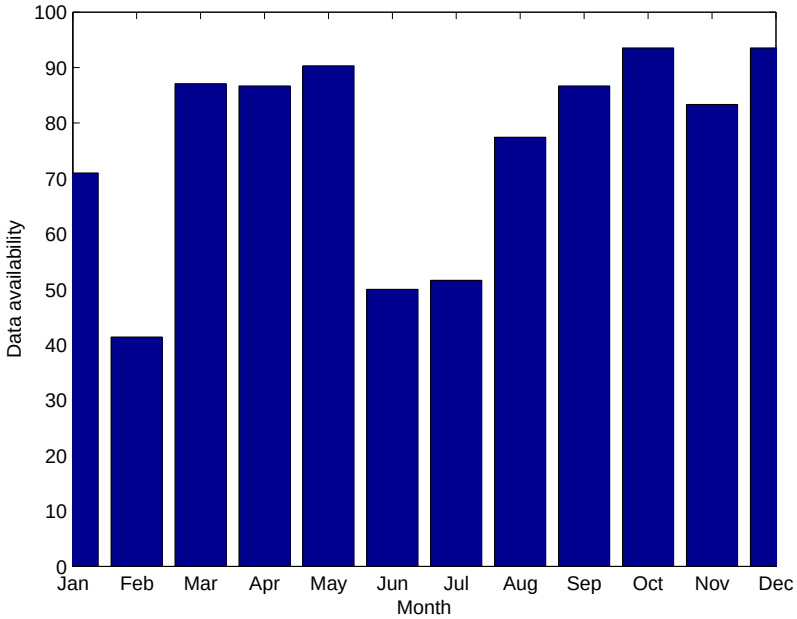

Figure 5.15: A graph showing the availability of training data for Cachoeira Paulista in 1980.

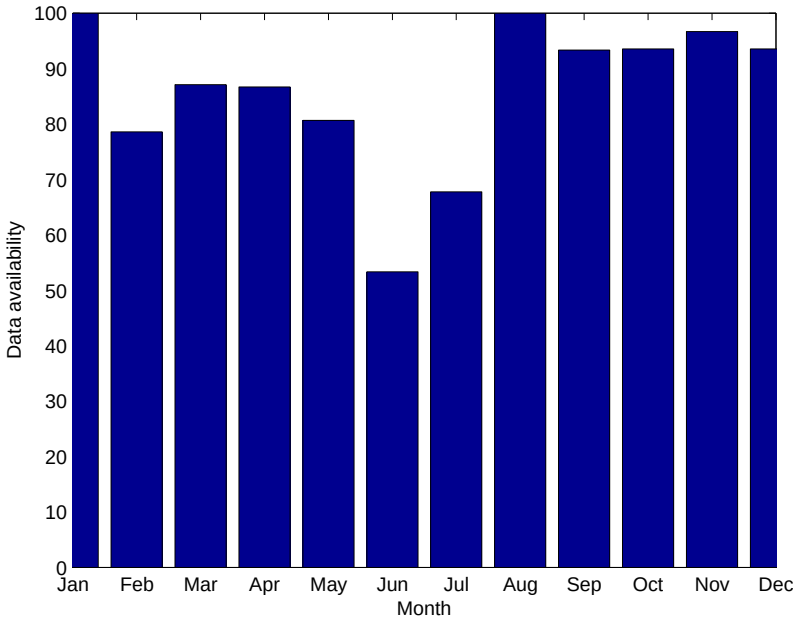

Figure 5.16: A graph showing the availability of training data for Cachoeira Paulista in 1985.

No data was available from May to September 1985 at Fortaleza. There was also an absence of spread F data from May to June in 1986, 1987 and 1988. This absence of spread F data during the winter months is most likely the cause of the poor performance of the BSNN model during winter months at Fortaleza. In addition, the continuous availability of spread F data at Cachoeira Paulista is most likely the reason for the excellent performance of the BSNN model at Cachoeira Paulista.

The aim of a NN model is to find the best average solution to a given problem, and if there is no data for training for a certain section of the input space the NN has a hard time generalising the solution, and the result is that the NN performs poorly in those under-represented areas. A NN interpolates well but does not extrapolate well.

5.5 Abdu model vs BSNN model

This section presents a comparison of the BSNN model results and the Abdu model (Abdu *et al.*, 2003) results for the year 1989. The Abdu model was developed using the monthly spread F occurrence statistics, derived from the same data as that used in this research. Its output is the monthly probability of spread F occurrence. It therefore follows that the Abdu model provides a better comparison with the BSNN model. The inputs to the Abdu model are the day number and solar flux (F10.7). Equation 5.4 was used to compute the magnetic latitudes using the magnetic declination values for Cachoeira Paulista and Fortaleza, and the results are presented in Table 5.1. The Abdu

Table 5.1: Magnetic latitude values for 1989

Month	Cachoeira Paulista	Fortaleza
January	-15.505	-3.695
February	-15.523	-3.714
March	-15.539	-3.733
April	-15.556	-3.751
May	-15.574	-3.770
June	-15.583	-3.780
July	-15.591	-3.789
August	-15.608	-3.808
September	-15.625	-3.826
October	-15.642	-3.845
November	-15.660	-3.863
December	-15.677	-3.882

spread F model code was used to determine the probability of spread F. The day number corresponding to mid-month and the average monthly solar flux (F10.7) were used as inputs for the months considered. The months selected for a comparative analysis covers autumn equinox (March), winter solstice

(June), spring equinox (September) and summer solstice (December). The Abdu model was then used to predict the spread F probabilities for these selected months during the year 1989 (high solar activity). The probabilities of spread F were then expressed as percentages.

Data corresponding to magnetic latitudes -15.0 and -3.75 degrees were considered for Cachoeira Paulista and Fortaleza respectively. The actual magnetic latitude for Cachoeira Paulista was not considered due to the limitation of the Abdu model which is designed to work within the limits from -15.0 to +15.0 degrees. An average magnetic latitude of -3.75 was chosen for Forteleza. Experimentation showed that differences of 0.5 in magnetic latitude did not significantly affect the model results.

The results from the comparison are shown in Figure 5.17, where the blue coloured triangles refer to the probability of spread F given by the Abdu model. The red coloured dots refer to the probability of spread F as observed on ionograms while the green coloured plus signs refer to the probability of spread F as predicted by the BSNN model.

The results for spring equinox (March 1989) indicate that both the BSNN and the Abdu models predict higher than observed probabilities during the early morning hours for Fortaleza station. During the same month at Cachoeira Paulista, the Abdu model predicts probabilities of spread F during the night hours that are more than 50% higher than observed ones, while the BSNN model predicts results that are within 20% of the observed probabilities of spread F.

The results for the winter solstice (June 1989) show that the BSNN model predicts higher than observed spread F probabilities during the early morning hours at Fortaleza, which could be due to a lack of winter data available for training from this station as explained in the previous section. Both models predicted the probabilities of spread F within 15% of the observed probabilities at the low latitude site Cachoeira Paulista.

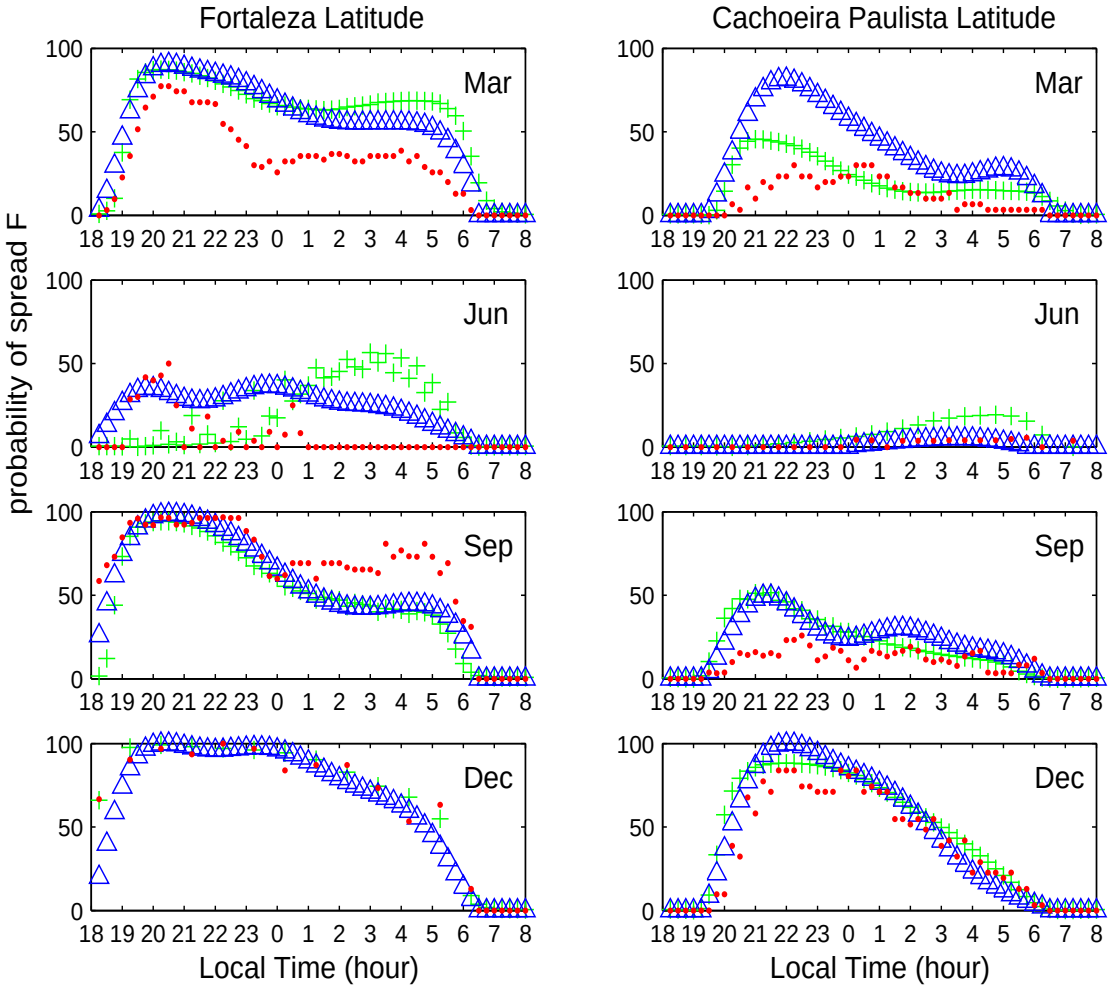

Figure 5.17: A comparison of the two models with observed probability of spread F for March, June, September and December 1989.

For the spring equinox (September 1989), both models predict within 20% of the observed probabilities during the post sunset hours and $20-30\%$ below the observed probabilities during the early morning hours for Fortaleza. The trend in spread F onset time and the times of peak probability are within one hour of the observed onset and peaks. For the summer solstice (December 1989), both models predict the probabilities of spread F within 10% of observed probabilities.

5.6 Summary of results

The BSNN model results presented in this chapter show that the occurrence of spread F can be predicted using a model developed with the technique of NNs. The BSNN model performs to the same extent as with the Abdu (Abdu *et al.*, 2003) model. The results also show that spread F is a night-time phenomenon with a peak onset time around 19:30 LT at Fortaleza and around 21:00 LT around Cachoeira Paulista. The later onset time at Cachoeira Paulista (CP), which is further away from the equator, is possibly due to the vertical growth time for the field line aligned plasma bubble structures over the equator, given the fact that spread F over CP occurs when the equatorial apex of the bubble field line maps to the F layer bottom side over CP.

The results show that on average, throughout all seasons, range spread F is more likely at the equatorial latitudes than at higher latitudes, thereby supporting the generalization that range spread F is an equatorial ionospheric phenomenon. The BSNN model results indicate a high spread F activity during the spring through to autumn months with peak probability in summer centred around December. Winter months have the least spread F activity.

An analysis of the difference in predicted and observed probabilities shows that the BSNN model performs within 30% of observations in making the required predictions for all but the winter season at Fortaleza. The huge gaps in data from 1985 to 1988 during the winter months at Fortaleza are thought to have contributed to the poor performance of the BSNN model during that period.

A comparative analysis of the BSNN and Abdu model results shows that the BSNN model performs to the same extent as the Abdu model for the months considered.

Chapter 6

Discussion and conclusions

6.1 Introduction

This chapter presents a discussion on the research described in this thesis, a summary of the results found and a proposal for future work on spread F predictions using the technique of NNs. The aim of this study was to develop a NN based model to predict the occurrence of spread F using ionosonde measurements from the Brazilian region. Results obtained show that NNs are suitable for spread F predictions with the following input parameters: geographic latitude (lat), magnetic declination (dec) and inclination (inc), day number (DNS and DNC), hour (HrS and HrC), a 3-month running mean of the daily sunspot number (R_3) and the running mean of the previous eight 3-hourly magnetic Ap index values (A_8).

6.2 Discussion

The Rayleigh-Taylor (R-T) instability mechanism is widely believed to cause ionospheric spread F irregularities. The linear growth rate for the R-T instability suggests that many competing processes are responsible for the generation of spread F. Spread F occurrence has been extensively studied in terms of the monthly percentage occurrence. To date, the diurnal, seasonal and solar cycle variability in spread F occurrence is fairly well characterised

statistically. However, the day to day variability in spread F remains the least understood (Abdu *et al.*, 1999).

Because of the spread F data format used in this study, the occurrence of spread F was represented by a measure equal to one while the absence of spread F was represented by zero. As outputs to the NN, a measure between zero and one were given by the NN, representing the occurrence of spread F. For the purpose of this research, the NN results were expressed as the probability of spread F, which also allowed for a comparative analysis with an alternative empirical model designed for the same purpose. The results presented in this thesis confirm the findings of Abdu *et al.* (2003). According to statistical analysis of the occurrence of different types of spread F, the probability of frequency spread F is slightly higher for lower latitude station Fortaleza, but evidently less significant comparing with the probability of range spread F.

One of the major drawbacks in spread F forecasting is the reliance on a single spread F measuring technique to come up with the spread F model dataset, in the case of the data used in this thesis, ionogram detected spread F. The use of HF radar (Cecile *et al.*, 1996), scintillation data, ground-based optical measurements and satellite topside sounders may help to come up with a dataset that will unambiguously identify the different types of spread F and most importantly the "age"of plasma bubbles. This will help to confirm one of the widely held views that post-midnight spread F is not entirely due to the unstable or potentially stable local plasma but due to the overhead passage of irregularities originating from either the east or west of the observation site. This will help in determining the actual spread F onset conditions.

Abdu *et al.* (1999) explain in detail that the day-to-day variability is controlled by the origins of spread F seeding perturbation source which initiates the RT instability. Several factors, including the direction and amplitude of seeding factors like gravity waves, have been cited as main causes of the day-

to-day variability. This is however notwithstanding other factors including the equatorial ionisation anomaly, which has been found to strengthen in the afternoon of spread F days. Other key factors in understanding the origin of spread F are the F layer height and the vertical plasma drift.

It therefore follows that the inclusion of the abovementioned parameters into the NN input space may help to improve the NN model's performance on the day-to-day predictions of the onset times and some rapid variations during individual nights.

6.3 Summary of results

The following is a summary of the results obtained:

- A NN with two hidden layers and thirty hidden nodes was found to be optimal for spread F predictions.
- The seasonal (DNS and DNC), diurnal (HrS and HrC), magnetic activity (A_8, a running mean of the previous eight 3-hourly Ap index values) and solar activity (R_3, a three-month running mean of the sunspot number) were determined as optimum for spread F predictions for single station models.
- An initial single station model was developed with range and frequency spread F data from Fortaleza. After a comparison of range and frequency spread F occurrence at the two Brazilian stations, the occurrence of frequency spread F alone was taken as an absence of range spread F and only range spread F data was used to develop single station models. FSNN and CPNN were developed for Fortaleza and Cachoeira Paulista respectively, the results from these models were presented and discussed.
- In addition to the above single station model parameters, a regional spread F model (BSNN) was developed with geographic latitude (lat),

magnetic declination (dec) and inclination (inc) as additional input parameters.

- A comparative analysis of the BSNN and the Abdu (Abdu *et al.*, 2003) models has shown that NNs can be used to predict the occurrence of spread F.

6.4 Future work

This study was restricted to two locations within Brazil. Future work will include investigating other locations around the world, particularly near the geomagnetic equator and using solar radio flux F10.7 index instead of sunspot number for it has been used as an input to other existing spread F model. Another important consideration will be the day-to-day variations of spread F. Factors that are believed to cause the daily variability including the equatorial ionisation anomaly, vertical plasma drift, gravity waves, thermospheric winds and F2 layer height, and these will be considered in the input space for spread F predictions in an attempt to model the daily variability. Other sources of spread F data need to be considered in cases where ionosonde data is not available in order to archive a large dataset covering a wide area, which will provide a more uniform representation of spread F occurrence for NN modelling.

In conclusion, this thesis has shown that NNs may be used to develop a prediction tool for the occurrence of spread F, however, substantial effort is required to improve the database available and refine the inputs known to influence spread F occurrence.

References

Abdu M.A., Sobral J.H.A. and Batista I.S. "Equatorial spread F statistics in the American longitude: some problems relevant to ESF description in the IRI scheme". Advances in Space Research, vol. 25(1), pp. 113 – 124, 1999.

Abdu M.A., Souza J.R., Batista I.S. and Sobral J.H.A. "Equatorial spread F statistics and empirical representation for IRI: A regional model for the Brazilian longitude sector". Advances in Space Research, vol. 31(3), pp. 703 – 716, 2003.

Bowman G.G. and Mortimer I.K. "Ionospheric coupling, especially between ionogram-recorded spread-F and sporadic-E enhancements at an equatorial-anomaly crest station, Chung-Li". Journal of Geophysical Research, vol. 107(A10,7), pp. 1 – 6, 2002.

Cecile J.F., Vila P. and Blanc E. "HF radar observations of equatorial spread-F over West Africa". Annales Geophysicae, vol. 14, pp. 411 – 418, 1996.

Chen W.S., Lee C.C., Liu J.Y., Chu F.D. and Reinisch B.W. "Digisonde spread F and GPS phase fluctuations in the ionosphere during solar maximum". Journal of Geophysical Research, vol. 111, pp. 1 – 9, 2006.

Cox A. and Hart R.B. *Plate Tectonics: How it works.* Blackwell Publishing, Palo Alto, CA, 1996.

Das A.C. *Space Plasma Physics, an introduction.* Narosa Publishing House, New Delhi, 2004.

Davis K. *Ionospheric Radio*. Peter Peregrinus Ltd, United Kingdom, iee electromagnetic waves series 31 edn., 1990.

Fagundes P.R., Sahai Y., Batista I.S., Abdu M.A., Bittencourt J.A. and Takashi H. "Observations of day-to-day variability in precursor signatures to equatorial F-region plasma depletions". Annales Geophysicae, vol. 17, pp. 1053 – 1063, 1999.

Fausett L. *Fundamentals of Neural Networks, architectures, algorithms, and applications*. Prentice Hall International, Inc, New Jersey, 1994.

Habarulema J.B., McKinnell L.A. and Cilliers P.J. "Prediction of global positioning system total electron content using Neural Networks over South Africa". Journal of Atmospheric and Solar-Terrestrial Physics, vol. 69(15), pp. 1842 – 1850, 2007.

Haldoupis C., Kelley M.C., Hussey G.C. and Shalimov S. "Role of unstable sporadic-E layers in the generation of midlatitude spread F". Journal of Geophysical Research, vol. 108(A12, 11), pp. 1 – 8, 2003.

Haykin S. *Neural Networks, A comprehensive foundation*. Macmillan Publishing Company, Englewood cliffs, New Jersey, 1994.

Huang C.S. and Kelley M.C. "Nonlinear evolution of equatorial spread F, Gravity waves, velocity shear, and day-to day variability". Journal of Geophysical Research, vol. 101(A11, 24), pp. 521 – 532, 1996.

Huang C.Y., Burke W.J., Machuzak J.S., Gentile L.C. and sultan P.J. "Equatorial plasma bubbles observed by DMSP satellites during a full solar cycle: Toward a global climatology". Journal of Geophysical Research, vol. 107(A12, 7), pp. 1 – 6, 2002.

Huba J.D., Bernhardt P.A. and Ossakow S.L. "The Rayleigh-Taylor instability is not damped by recombination in the F region". Journal of Geophysical Research, vol. 101(A11, 24), pp. 553 – 556, 1996.

Hysell D.L. and Shume E.B. "Electrostatic plasma turbulence in the topside equatorial F region ionosphere". Journal of Geophysical Research, vol. 107(A10, 1), pp. 1 – 12, 2002.

Jayachandran P.T., Ram P.S., Somayajulu V.V. and Rao P.V.S.R. "Effects of equatorial ionization anomaly on the occurrence of spread-F". Annales Geophysicae, vol. 15, pp. 255 – 262, 1997.

Kelley M.C. *The Earth's Ionosphere, plasma physics and electrodynamics.* Academic Press, Inc, San Diego, Califonia, 1989.

Kelly M.C., Makela J.J., Ledvina B.M. and Kintiner P.M. "Observations of equatorial spread-F from Haleakala, Hawaii". Geophysical Research Letters, vol. 29(20, 64), pp. 1 – 4, 2002.

Le G., Huang C.S., Pfaff R.F., Su S.Y., Yeh H.C., Heelis R.A., Rich F.J. and Hairstone M. "Plasma density enhancements associated with equatorial spread F: ROCSAT -1 and DMSP observations". Journal of Geophysical Research, vol. 108(A8, 3), pp. 1 – 14, 2003.

Lee C.C., Liu J.Y., Reinisch B.W., Lee Y.P. and Liu L. "The propagation of traveling atmospheric disturbances observed during the April 6 -7 ionospheric storm". Geophysical Research Letters, vol. 29(5, 12), pp. 1 – 4, 2002.

McKinnell L.A. and Poole A.W.V. "A neural network based electron density model for the E layer". Advances in Space Research, vol. 31(3), pp. 589 – 595, 2003.

Ossakow S.L. "Spread F theories - a review". Journal of Atmospheric and Solar Terrestrial Physics, vol. 43(5/6), pp. 437 – 452, 1981.

Sastri J.H. "Post-midnight onset of spread-F at Kodaikanal during the June solstice of solar minimum". Annales Geophysicae, vol. 17, pp. 1111 – 1115, 1999.

Subbarao K.S.V. and Murthy B.V.K. "Seasonal variation of equatorial spread - F". Annales Geophysicae, vol. 12, pp. 33 – 39, 2006.

Sultan P.J. "Linear theory and modeling of the Rayleigh- Taylor instability leading to the occurrence of equatorial spread F". Journal of Geophysical Research, vol. 101(A12, 26), pp. 875 – 891, 1996.

Williscroft L.A. and Poole A.W.V. "Neural networks, foF2, sunspot number and magnetic activity". Geophysical Research Letters, vol. 23(24), pp. 3659 – 3662, 1996.